REVIEW

Review on all-optical logic gates: design techniques and classifications – heading toward high-speed optical integrated circuits

Erandathara Gokulan Anagha and Ramasamy Kandasamy Jeyachitra*
National Institute of Technology, Department of Electronics and Communication Engineering, Tiruchirappalli, Tamil Nadu, India

Abstract. All-optical logic gates (AO-LGs) are the key elements that play a pivotal role in the development of future all-optical networks and all-optical computing. A complete overview of the seven all-optical logic gates (i.e., AND, OR, NOT, XOR, XNOR, NAND, and NOR) based on their design techniques and applications are covered, including the latest technologies, such as topological photonics and artificial intelligence-based designs techniques. In addition, we have further categorized the AO-LGs as reconfigurable gates, simultaneous gates, reversible gates, modulation-based gates, and data rate-based gates. The techniques to implement these different classes of gates are reviewed and their limitations are discussed. We also discuss in brief the various simulation tools used to design and analyze the AO-LGs. Finally, the most feasible techniques for constructing optical integrated circuits based on the existing fabrication technologies and available resources are explored, and future prospects are outlined. [DOI: 10.1117/1.OE.61.6.060902]

Keywords: all-optical logic gate; optical integrated circuits; reconfigurable logic gates; simultaneous logic gates; reversible logic gates.

Paper 20220186V received Feb. 25, 2022; accepted for publication May 24, 2022; published online Jun. 25, 2022.

1 Introduction

Currently, the increasing demands for higher bandwidths and ultrafast operating speed requirements imposed by the internet-based variety of applications have created the electronic bottle neck problem. These needs have overloaded the available bandwidths and reached the speed limits of electronic-based devices. This calls for a quick shift toward a newer technology that can meet the demands of high speed and abundant bandwidth to keep pace with the user demands. Compared with electrons, light or photons have several advantages. It has much greater speeds, can carry a huge amount of information, and can provide terahertz range of bandwidths. Further, the interactions between photons are not as strong as that of electrons and hence they reduce energy losses in addition to providing immunity from electromagnetic interferences and ground loops. Despite using optical fiber cables for communication systems, the conversions from optical to electrical and vice versa decreases the speed of operation and hence, the full capacity of optical systems cannot be utilized. Thus, all-optical signal processing, all-optical devices, and a complete optical network have been identified as the potential candidate to replace the conventional electronic integrated circuits.

To form a complete optical network, all the operations from signal generation, processing, encoding, modulation, transmission, demodulation, decoding, filtering, and so on have to be performed in a fully optical manner. The various electronic based devices for performing these actions must be switched into a complete optical domain. This calls for all-optical logic gates (AO-LGs), all-optical sequential and combinational circuits, all-optical processors, and so on. For developing such optical circuits, the design of AO-LGs is a prerequisite. There are various design aspects to be considered in the design of such gates. Designing of AO-LGs suitable for optical integrated circuits (OICs) requires features, such as high contrast ratio (CR), low response times, small dimensions, and low power consumption.[1] It should be simple and offer

*Address all correspondence to R. K. Jeyachitra, jeyachitra@nitt.edu

compatibility with hybrid optoelectric systems and the future all-optical systems without compromising the speed of operation.

In this paper, a complete review of the existing techniques for implementing AO-LGs are explored and their limitations and possible solutions are discussed. An outline of the proposed review paper is given in Fig. 1. We have categorized the logic gates based on their basic techniques of implementation which includes design of the various categories of AO-LGs as shown in Fig. 2. This is covered in Sec. 2. Based on their operation, two classes of AO-LGs are identified as reconfigurable gates and simultaneous gates. The advantages of these types of gates and their implementations are described in Sec. 3. Further, some designs of AO-LGs are focused on the modulation format and data rates in specific. Such designs are analyzed in Sec. 4. Section 5 presents the design of AO-reversible logic gates and their features. In the next section, the various

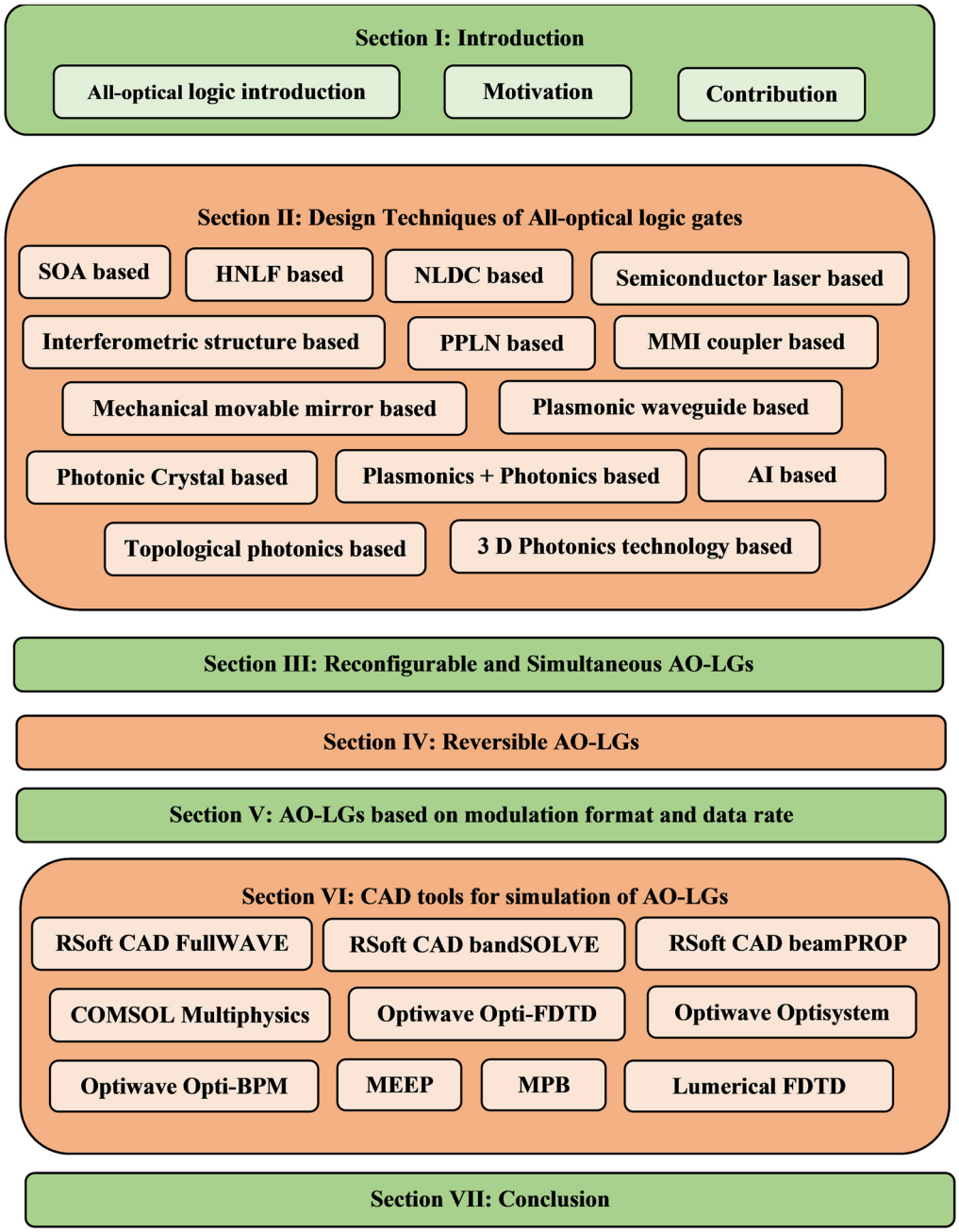

Fig. 1 Outline of the proposed review paper.

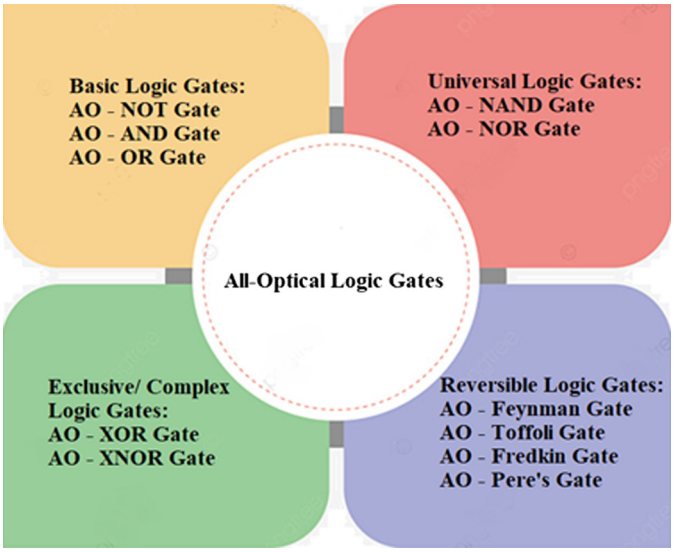

Fig. 2 Classification of AO-LGs.

applications of AO-LGs and their design techniques are outlined. Section 7 provides a brief summary of the working principle of various techniques used for designing AO-LGs. In Sec. 8, the various CAD tools for the simulation of AO-LGs are discussed in short. Section 9 focuses on the current status and challenges faced by photonic integrated circuits and future prospects. This is followed by conclusion in Sec. 10 and the detailed list of references.

2 Design Techniques of AO-Logic Gates

The seven AO-LGs namely NOT, AND, OR, NAND, NOR, XOR, and XNOR gates are irreversible gates. These are the most widely used logic gates in the construction of sequential and combination logic circuits for a wide variety of applications.

2.1 *SOA-Based Designs*

Among the different techniques of implementations, semiconductor optical amplifier (SOA)-based designs are the earliest ones. The initial designs utilized the cross-phase modulation (XGM) effect alone in SOA structures.[2] Here, the input signal was used to saturate the gain and thus modulate a probe signal to achieve the desired output signal. The designs based on XGM alone was simpler, polarization-independent, and provided feasibility of bit rates up to 100 Gbps. However, due to the large gain modulation, the requirements of high pump power for nonlinearity, formation of large chip output, and bulky designs were the shortcomings that lowered their performance. An experimental demonstration of AO-AND gate utilizing cross polarization modulation in SOA was performed with a CR of around 16 dB as shown in Fig. 3(a). This design

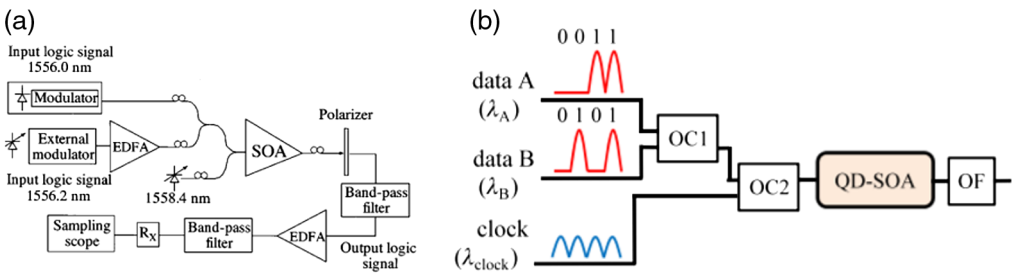

Fig. 3 (a) Experimental demo of AO-AND gate using SOA.[3] (b) Configuration of AO-NOR using single QD-SOA.[4]

differed from the previous SOA-based designs in generating an output signal with a wavelength independent of that of the input signals.[3] To achieve better results, SOAs were combined with interferometric configurations thereby utilizing cross phase modulation (XPM) effect. SOA with Michelson interferometers were designed as these gates have simpler structure since they offer direct access for the input signal to the SOAs.[5] AO-XOR gate operating at 20 Gbps was experimentally verified using SOA-based ultrafast nonlinear interferometer (UNI) switch.[6]

The most widely used configuration for the realization of AO-logic gates is the Mach Zehnder interferometric configuration (MZI) due to its attractive features, such as low energy requirement, low latency, and high stability. AO-OR gate was designed using SOA-MZI at 10 Gbps.[7] By utilizing a delayed interferometer (DI) along with SOA-MZI configuration, AO-XOR operation was achieved 80 Gbps.[8] It was observed that the quality of XOR operation was improved by the addition of DI. A more practical and matured design using the principle of DI was proposed recently by masking the longer SOA recovery time to realize AND, NOR, XNOR gates at 160 Gbps with high Q factor.[9] Another approach toward SOA-based AO-LG design is based on terahertz optical asymmetric demultiplexer (TOAD) by utilizing its low levels switching energy to achieve precise control of signals. An AO-XOR gate for nonreturn to zero (NRZ) signals based on TOAD was experimentally demonstrated.[10] SOA with fiber Sagnac interferometer was utilized to experimentally demonstrate AO-XOR operation at 10 Gbps and AO-AND gate at 100 Gbps.[11,12] This scheme was able to weaken the influence of carrier recovery time of SOA on the logic gate operation compared with TOAD-based design, however, stability remained a drawback. In addition to XPM and XGM effects, four-wave mixing (FWM) was also utilized in SOA-based design. However, two pump signals are required to ensure polarization-independent operation of such gates and owing to the complexity of pumping schemes, and it can be used only for higher bit rates (>100 Gbps). AO-NOR gate was realized using FWM effect in SOA, with feasibility of possible integration.[13]

More recent designs utilize carrier reservoir SOA (CR-SOA), quantum dot SOA (QD-SOA), photonic crystal SOA (PC-SOA), and reflective SOA (RSOA)-based approaches. AO-OR gate design using CR-SOA with DI achieved 100 Gbps operation with a Q factor of 9 by overcoming the SOA response limitations.[14] AO-NAND and XNOR gates were realized for the first time at 120 Gbps for return to zero (RZ) data using CR-SOA.[15] Owing to the relaxed structural conditions and flexibility of photonic crystal devices, PC-SOA-based AO-NOR and AO-XNOR gates provided better performance compared with conventional SOA designs.[16] Such designs were found to provide highly improved performance characteristics when high data rates are required with high PRBS lengths compared with conventional SOA-based approaches. RSOA consists of a high-reflectivity covering on one side and antireflectivity coating to another side and possesses advantages such as higher gains for lower bias currents and faster response with reduction in cost and complexity of designs compared with conventional SOA approaches. AO-XOR gate using RSOA achieved 300 Gbps at 0.3 mW power input.[17] SOAs having quantum dot active regions or QD-SOAs provide superior performance compared with their conventional counterparts owing to their high thermal stability, low temperature sensitivity along with ultrafast gain recovery times. AO-AND, XOR, and NOT gates were modeled using QD-SOAs to operate up to 250 Gbps. However, it was observed that for better results, higher injection currents and narrow input pulse widths were required.[18] By utilizing the advantages of XPM and XGM in cascaded QD-SOA structures, AO-NAND gate with extinction ratio (ER) of 163 dB at 640 Gbps was realized.[19]

Another approach with a series configuration of QD-SOAs to realize AO-NAND operation was numerically simulated at 1 Tbps with the feasibility of achieving high Q factor even with the effects of amplified spontaneous emission noise.[20] A numerical model for simulating AO-XOR and AND gates using two photon absorption (TPA)-induced pumping to reduce pattern effects leading to high Q factor with 320 Gbps operation was proposed.[21] Another approach using a single QDSOA with an optical filter was utilized to achieve AO-NOR operation at 160 Gbps as shown in Fig. 3(b). However, an additional clock signal was utilized as a probe, which imposed some challenges, such as synchronization and generation.[4] The power consumption in QDSOA-based devices is still a drawback that limits its compatibility for use in integrated circuits.

A possible alternative is to utilize the slow light phenomenon of photonic crystal waveguides to bring down the power consumption of QD-SOAs in addition to enhancing the gain and phase

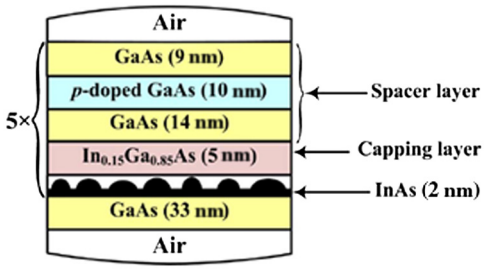

Fig. 4 Active region of PC-QDSOA.[22]

changes. Such designs enable precise confinement and efficient transmission of light signals and lead to compact and feasible realizations. AO-NOR gate based on PC-QDSOA with a low power consumption of 4 mW was realized with the low ER of 7 dB limited by the slow phase recovery of PC-QDSOAs.[22] Figure 4 shows the active region of the proposed PC-QDSOA. A similar realization achieved AO-OR and AND operations at 160 Gbps with Q factors.[23]

2.2 *Nonlinear Fiber-Based Design*

Few of the earlier designs of AO-LGs besides SOA were based on the nonlinearity of the optical fiber itself. Highly nonlinear fiber (HNLF) has the ability to process ultrafast signals by utilizing the Kerr effect in silica, and the requirements of high input powers for nonlinearity and bulky dimensions (longer interaction lengths) limited their use in integrated circuits. AO-XOR gates were implemented using nonlinear polarization rotation in HNLF at 20 Gbps.[24] An experimental demonstration of AO-XOR, NOT, and AND gates using nonlinear polarization rotation in HNLF was performed at 10 Gbps.[25,26] Among the earlier designs, some implementations were based fully on optical fiber componenets and nonlinearity, such as nonlinear directional couplers as shown in Fig. 5, asymmetric couplers, and so on. Various AO-LG operations were numercially analyzed using a symmetric three-core nonlinear directional coupler (TNLDC) and an asymmetric two-core coupler (DNLDC) and their performances were compared by introducing a new figure of merit.[27] AO-AND, XOR, and OR gates were analyzed based on three different asymmetric DNLDC with varying self pahse modulation (SPM) profiles wherein the optimization of nonlinearity profile lead to better results.[28] By utilizing soliton propagation in TNLDC, AO-XOR, OR, NAND, NOR, XOR, and XNOR gates were analyzed numerically.[29]

2.3 *Interferometer-Based Design*

There are several designs of AO-LGs based on interferometric structures, such as MZI, Sagnac interferometers, and UNI. The basic principle behind such structures is the interaction between different waves leading to constructive or destructive interfernce depending on phase, amplitude, and frequency (wavelength) of the waves. Nonlinear effects commonly utilized with such structures for the design of AO-LGs include XPM, two-photon absorption, etc. Nonlinear optical loop mirror (NOLM) or the nonlinear Sagnac interferometer was used in the early designs of AO-LGs.

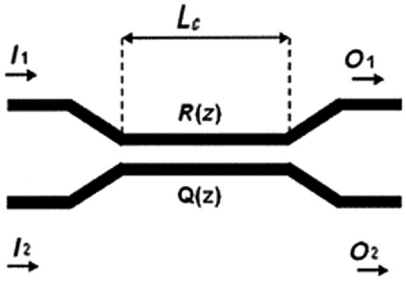

Fig. 5 A nonlinear directional coupler of length *Lc*.[27]

Owing to its inherent stability and fast response times due to fiber nonlinearity, such designs provided feasibility for all-optical signal processing. However, NOLM requirements of high optical powers and longer fiber lengths restricted their flexibility and widespread use. AO-XOR operation was experimentally demonstrated at 10 Gbps using a fiber Sagnac interferometer assisted by SOA.[11] Another such work realized AO-LGs using low birefringent NOLMs at 100 Gbps for the application of all-optical packet drop function.[30] Electro-optic effect-based cascaded MZI structures were used to achieve XOR, XNOR, AND functionalities.[31] Various logic functions were realized using local nonlinear MZI acting as a phase shifter employing angular deflection of spatial solitons.[32] Few of the recent works utilized photoic crystal-based nonlinear MZI wherein the nonlinear arm of MZI is replaced with slotted photonic crystal waveguide. By utilizing a control signal and XPM phenomenon, an AO-NOT with low input power requirement and response time of 3 ps was succesfully implemented.[33] Another approach used MZI with dual-core nonlinear photonic crystal fiber (PCF) to achieve AND and OR gates having high CR.[34] Some of the experimental works on AO-LGs were based on semiconductor laser diodes with the target of lowering response times and cost effective approaches. AO-NOT and NOR gates were experimentally demonstrated at 10 Gbps by utilizing the gain modulation technique in Fabry–Perot laser diodes (FP-LDs). This technique provided the added advantage of supporting multicasting operation of AO-LGs with low power operation and high ER.[35] Similar realization of AO-NOT and NOR gates at 10 Gbps with FP-LDs allowing two different wavelengths was achieved with the possibility of attaining up to 40 Gbps speed by replacing with quantum-well FP-LDs.[36] A much simpler design without using any external probe signals was achieved based on a single mode FP-LD working on self-locked dominant mode to achieve NAND, XNOR, AND, and XOR operations at 10 Gbps.[37] Recently, a hybrid cavity semiconductor laser consisting of a FP cavity and a square microcavity was used to experimentally demonstrate NOT, NOR, and NAND functions at 20 Gbps with high ER values.[38]

2.4 *PPLN-Based Design*

Periodically poled lithium niobate (PPLN) waveguides were utilized to realize all-optical logic functions with ultrafast response, complete transparency, negligible spontaneous emission noise, independency of data format, and bit rate and low intrinsic frequency chirp. However, size limitations along with temperature and polarization dependencies limit their use in integrated circuits. Based on sum-frequency generation in a single PPLN waveguide, AO-OR and XOR gates were realized at 40 Gbps.[39] An experimental demonstration of AO-AND gate based on cascaded sum and difference frequency generation in PPLN waveguide was performed at 20 Gbps.[40] Electro-optic effect in PPLN was utilized to achieve AO-controlled NOT, XNOR, and XOR gates based on polarization control with experimental demonstration.[41] By utilizing the mechanical movement of mirrors, the path followed by light signals can be controlled in a suitable manner to achieve all-optical logic operations.

2.5 *MEMS and Nematic Liquid Crystal-Based Design*

Three variable AO-XOR and XNOR gates were implemented with mechanical movable mirrors with feasibility of chip-level implementation using MEMS (micro electromechanical systems)-based systems.[42] A liquid crystal light valve with a photonic crystal slab was utilized to achieve all-optical control of spatial solitons for the realization of reconfigurable AO-LGs. AO-NOR and XNOR functions were achieved in such a manner using external beams for flexible operations.[43] Despite possessing longer response times, the generation of solitons in nematic liquid crystals to perform all-optical logic operations has advantages such as transparent spectrum and nonresonant nonlinearity which may be explored further.

2.6 *MMI-Based Design*

Multimode interference (MMI)-based devices work on the principle of self-imaging to achieve the desired logic operation wherein the guided modes of the MMI region are excited to interfere constructively. AO-XOR, NAND, OR, XNOR, and NOT gates were realized using an MMI

waveguide structure with compact dimensions with simultaneous operations.[44] A 3-dB MMI coupler was used to implement a two-input AO-XOR gate as a base structure for the design of three- and four-input XOR gates and addressed the possible fabrication issues for practical implementations.[45] AO-AND, OR, NOR, and XOR gates were realized based on MMI effect using 2×2 MMI couplers.[46]

2.7 *Plasmonic Waveguide-Based Design*

Plasmonics and photonics are two widely researched areas with regard to the design of AO-LGs due to their fascinating features that enable flexible, compact, and ultrafast realizations. Plasmonic slot waveguides exhibit strong plasmonic enhancement enabling strong confinement of light into a subwavelength range region and possess ultralong range propagation over several micrometres. To overcome the limitations in performance, due to dust particles in the air slots, a possible solution of replacing air slots with dielectric has been utilized in several designs. AO-XNOR, XOR, NOT, and OR gates were realized using plasmonic slot waveguides based on linear interference with an ER of 24 dB.[47] Graphene-based plasmonic MZI structure was used to achieve 6 AO-LG functions with distinctive features, such as high flexibility, compactness, and large scalable bandwidth spectrum.[48] Hybrid metal on insulator metal plasmonic waveguide was utilized to realize AO-O, XOR, and NOT gates miniaturized dimensions and high ER of 26 dB based on interference effect.[49] A similar attempt was made recently with further reduced dimensions of using metal insulator metal (MIM) plasmonic waveguides and improved the CR value by 27.8 dB.[50] A simpler design for AO-AND gate was attempted using a Y-shaped MIM plasmonic waveguide with improved flexibility and operating speed.[51] The diffraction limit is a factor that brings down the photonics-based design approach when attempting compact designs with device dimensions comparable to operating wavelength. In such a scenario, plasmonics-based waveguides are better candidates, which helps in realizing ultracompact devices to overcome the diffraction limit and confine and control light in a precise manner.

2.8 *Photonic Crystal-Based Design*

Photonic crystals have recently emerged as the best platform for the design of all-optical logic devices with compact dimensions, high speed, simpler designs, flexibility, and compatibility with hybrid opto-electronic as well all-OICs. By utilizing their unique photonic bandgap property for efficient and precise control of light signals, several all-optical devices such as filters, multiplexers and demultiplexers, encoders and decoders, splitters, switches, logic gates etc. have been implemented.[52] In general, there are three approaches to design AO-LGs using photonic crystals. The first approach is based on linear effects which utilizes constructive and destructive interference effects and have much lower power consumption but require precise phase control, sometimes requiring external phase shifters. The disadvantage of this approach is that it is affected by phase sensitivity, operational bandwidth limitations, and low tolerance to input power fluctuations and therefore achieving high ER values is difficult. AO-AND, XOR, NOT gates using a Y-shaped photonic crystal waveguide based on interference effect with compact dimensions and reduced power consumption.[53] Another design realized AO-OR, NOT, AND gates based on wave optics theory with low response time of 0.128 ps.[54] The universal AO-NOR gate was recently designed using square lattice photonic crystals to bring down the delay time to 0.06 ps and enable easy fabrication and integration with OICs.[55] A power efficient design for AO-NOT gate using a nanoresonator in a hexagonal lattice of photonic crystals achieved a maximum data rate of 2.145 Tbps and verified the feasibility of operation in OICs as shown in Fig. 6(a).[1] The second approach is based on nonlinear effects which usually require longer interactions lengths and higher power consumptions to realize designs with high CRs with comparatively longer response times. Most of the available works utilize the optical Kerr effect wherein the refractive index of the pump signal is varied upon the application of high input intensity. Photonic crystal ring resonators working on Kerr effect were utilized to design AO- AND/OR/NOT gates with lower threshold input power at 1550 nm.[57] AO-AND gate with a response time of 0.4 ps with an input switching power of 10 W was proposed on GaAs substrate.[58] AO-NAND and NOR gates were realized with a unique bypass waveguide to reduce the heating effect in the

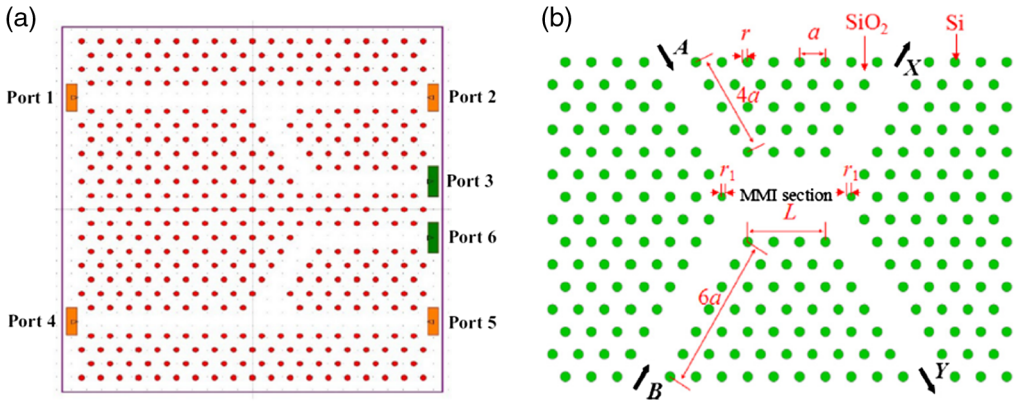

Fig. 6 (a) Checking the feasibility of photonic crystal AO-NOT gate in OICs.[1] (b) MMI-based photonic crystal LG design.[56]

integrated circuit with good CR values and low power consumption.[59] A GaAs-based photonic crystal ring resonator was utilized to achieve AO-AND operation using nonlinear Kerr effect with a response time of 1.8 ps.[60]

The third approach is based on self-collimation effect in photonic crystals with the advantage of intensity-independent operation. The interference between self-collimated beams were used to design AO-NOT, OR, AND, and XOR gates with low power consumption at the telecommunication wavelength of 1550 nm.[61] A 3-dB splitter based on line defects was utilized to realize AO-XOR and OR operations with a CR of 17 dB with simple design.[62] Various logic functions were achieved using a single structure based on silicon photonic crystals with compact dimensions and a CR value of 6 dB.[63] The limitations of using self-collimation effect is that dispersion control in photonic crystals is more difficult and it requires precise phase control with larger footprints. MMI effect has been utilized in photonic crystal waveguides due to their low loss, low polarization dependence, and wider bandwidths to realize AO-LGs with simple geometry. AO-XOR, NAND, XNOR, and OR gates were realized using MMI photonic crystal waveguide with ultra-compact dimensions of 6.9 μm $\times$ 6.7 μm and high CRs.[64] Various logic functions were realized on a BPSK modulated input signal using MMI waveguides in two-dimensional (2D) photonic crystals with a wide operating bandwidth of C band[56] as shown in Fig. 6(b). Si rods in a square lattice of photonic crystals are utilized to realize MMI-based AO-XNOR/XOR, OR/NAND gates with high CR of 40.41 and 37.40 dB with low response times of 0.131 ps and small footprint.[65] So far, most of the designs based on 2D photonic crystals utilized rods in air or any other substrate due to its simpler geometry and easy implementation. When considering the practical implementation and fabrication factors, photonic crystal slab-based designs come into the picture. Such designs provide confinement of light in vertical direction using total internal reflection and permit manipulation of light in the plane of slab. AO-NAND, AND, NOR, and OR gates were implemented on Ag-polymer photonic crystal slabs based on the nonlinear effects of the high Q-cavities.[66] On chip realization of AO-XOR, AND gates operating at different frequencies on silicon photonic crystal slabs were achieved without any nonlinear optical effects.[67] The seven major AO-LGs were realized using a 50:50 topologically protected beam splitter based on Si photonic crystal slabs with interference effect.[68]

2.9 *Photonics and Plasmonics Based Design*

Recently, several architectures utilizing the advantages of both plasmonics and photonics have come up to design AO-LGs. Hybrid plasmonic-photonic nanocavities possess the features of original cavities along with plasmonic features of metallic elements, which boosts the light matter interactions and offer better performance. One such design based on silicon insulator photonic crystal cavity equipped with a metallic nanoantenna was used to realize AO-NOT and AND logic functions.[69] AO-LGs were realized using triangular lattice of photonic crystals with copper-based plasmonic material as background material.[70]

2.10 *Topological Photonics-Based Design*

One of the recent technologies in use for the implementation of AO-LGs is based on topological photonics. The conventional photonic-based waveguides are not able to transport light over sharp turns (90 deg) without using a large radius of curvature. Also, the transmission cannot be achieved in an effcient way when defects are also included in such waveguide design. The nonnegligible backscattering in photonic crystal waveguides is a concern that requires some significant concern. In this case, a potential solution is the application of topologically protected edge states (TPES) in the anomalous Floquet photonic topological insulator structures, which enable easy fabrication. The advantage of this technology includes the ability to use visible light and extended spectrum upto near-IR for silicon photonics, efficient manipulation of optical signals, and robustness against disorder makes them potential candidates for AO-device design. AO-OR, AND, and XOR gates were implemented based on TPES in the visible light range for the first time along with the consideration of possible fabrication techniques.[71] A linear interference approach was utilized to implement the seven AO-LGs using 2D photonic crystals with edge states possessing advantages of immunity from disturbance and fault tolerance.[72] An experimental implementation of AO-OR/XOR gate based on coherent interactions between 1D photonic topological interfaces in coupled waveguide arrays was achieved with unique topological properties, such as efficient confinement, fast switching, and robustness.[73] A recent approach realized the various AO-LGs with high operational speeds utilizing metamaterials-based three-dimensional (3D) photonics technology by making suitable variations in diameter of air holes, lattice constant, and effective refractive index of the structure.[74] AO-OR, AND, and XOR gates were fabricated using 3D printing as simple, low-cost solutions to perform AO-logic operations at THz frequency ranges with possibility of reconfiguration to achieve various other logic functions.[75]

2.11 *Artificial Neural Networks-Based Design*

Another upcoming area of recent interest in the design of AO-LGs is based on artificial neural networks (ANNs). Most of the designs available in the literature so far depend on precise phase control of the incoming optical signals including their phase difference, polarization, and intensity. This makes the design of compact devices difficult due to bulky components or larger footprint requirements imposed by the phase control mechanisms.

Also, in practical scenarios, inaccuracy in phase control leads to instability and brings down the CR values which is the primary performance metric with regard to AO-LGs. To overcome these challenges, a universal strategy based on diffractive neural networks was proposed to realize the seven logic operations within a compact system using plane waves. After training, the diffractive neural network based on Huygen's metasurface could directionally scatter of focus light to designated areas to represent the two different logic states, 0 and 1. The proposed work possesses advantages such as universality of the design, powerful, and flexible operations and miniaturization. An experimental demonstration of the above concept performed at microwave frequencies to attain AO-NOT, OR, AND operations, and theoretical framework for their realization at terahertz frequencies was proposed.[76]

Most of the modeling techniques for AO-LGs utilize numerical simulations based on finite element method (FEM), finite difference time domain (FDTD), plane wave expansion (PWE), beam propagation method (BPM), and so on. The computational complexity and computation time of such simulators are still an open challenge that needs some addressing. Recently, ANN-based approaches have attempted to reduce the complexity, cost, and processing time and also improve the accuracy of output prediction. To simulate the performance and analyze the behavior of an AO-3 input XOR gate, two different approaches based on ANN were proposed. Two learning methods, multilayer perceptron and radial basis function, have been utilized to predict the output logic state of the proposed gate with improved accuracy and reduced processing times. This work opened up the possibility of exploring various machine learning-based algorithms to model AO-logic devices with high accuracy and bring down the computational time utilized by existing commercial softwares from several hours/minutes to the range of milliseconds.[77] Two optical neural networks composed of passive optical elements were utilized to achieve

Table 1 Summary of techniques for the design of AO-LGs.

Sl. no.	AO-LG design technique	Paper	Max data rate	Max CR (dB)	Remarks
1	SOA based	1 to 23,79	1 Tbps	19.21	Increased power consumption, bulky dimensions, and increased latency
2	HNLF based	24 to 26	20 Gbps	25	Increased power consumption, bulky dimensions
3	NLDC based	27 to 29	—	70.3	Bulky dimensions, lack of flexibility in design
4	Interferometric structure based	11, 30–34	100 Gbps	17	Bulky dimensions, phase control requirements, increased power consumption
5	Semiconductor laser based	35 to 38	20 Gbps	20	Bulky dimensions, high input power requirements
6	PPLN based	39–41	160 Gbps	—	Size limitations, temperature and polarization dependencies
7	Mechanical movable mirror based	42	—	—	Bulky dimensions, lack of integration capability and flexibility
8	Nematic liquid crystals	43	—	—	Size limitations, external phase control, longer delay time
9	MMI device based	44 to 46	—	26	Size limitations, excess loss, fabrication issues
10	Plasmonic waveguide based	47 to 51	3.33 Tbps	27.8	Propagation loss, flexibility
11	Photonic crystal based	1, 52 to 68	2.145 Tbps	40.41	Diffraction limit leading to size issues, power consumption for nonlinear effect-based designs
12	Plasmonics + photonics	69, 70	—	—	Able to overcome the diffraction limit and design ultracompact devices with precise control of light
13	Topological photonics based	71 to 73	—	>20	Signal loss at sharp bends in PhC waveguides can be overcome
14	3D photonics technology based	74, 75	—	—	Complexity, compatibility
15	Artificial intelligence based	75, 76, 78	—	—	Universal designs, miniaturization, flexible and powerful operation, complexity and computation time need to be addressed

AO-XOR operation with low power consumption.[78] A summary of the various techniques to design AO-LGs is shown in Table 1.

3 Reconfigurable and Simultaneous AO-LGs

In reconfigurable logic gates, more than one logic function can be realized without altering the device structure. The various logic functions can be realized by suitable techniques such as tuning the wavelength or using phase control. The advantage of reconfigurable AO-LGs is that they improve flexibility and robustness in addition to reducing the number of devices for integration in OICs. AO-NOR, AND, and OR gates were experimentally demonstrated at 100 Gbps using a single SOA along with an optical filter wherein reconfigurability was achieved by deployment of CW light and tuning of the optical bandpass filter at SOA output.[80] The experimental setup for

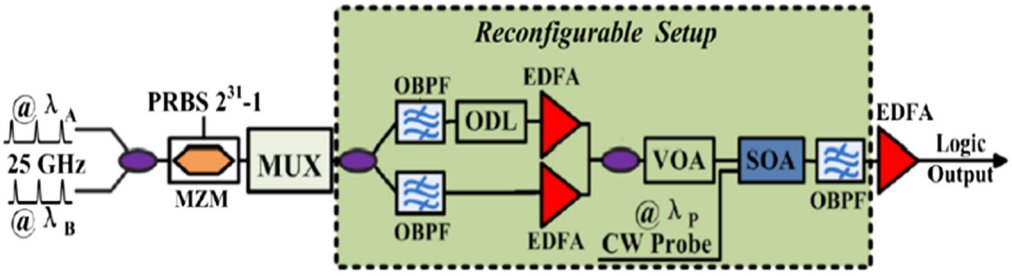

Fig. 7 Experimental setup for reconfigurable AO-LGs using single SOA at 100 Gbps.[80]

the same is shown in Fig. 7. Various AO-LGs were experimentally demonstrated for differential phase shift keying (DPSK) modulated signals at 20 Gbps utilizing SOA and delay interferometers. The variation of input wavelengths or phase control provided the required reconfigurability.[81] A Si photonic crystal-based compact structure operated as AO-XOR/NOT gate based on a fixed bias signal. The proposed device worked purely on linear optics regime and achieved high CR values with operating speed up to 3.15 Tbps.[82] A similar work based on photonic crystals achieved reconfigurable AO-XOR/OR gates by varying the phase of the input signals and achieved very low response time of 120 fs.[83] A reconfigurable structure to realize up to 25 logic functions by adjusting the bias voltage of the modulators, peak-to-peak voltages of the driving signals, and the rotation angle between the polarizations was simulated at 10 Gbps and experimentally verified to achieve the six basic logic functions at 1 Gbps.[84]

The unique photonic and optoelectronic properties and high confinement in graphene was utilized to design reconfigurable logic gates based on coherent perfect absorption principle in the THz region. AO-AND, OR, and XOR operations were achieved in a simple compact structure wherein switching between functions was achieved by varying the relative phase difference between the signals.[85] A QD-SOA and optical filter were utilized to achieve multiple logic operations on a single structure at 160 Gbps. The detuning of the filter was used to switch between NOT, OR, AND, and NOR operations with high quality output.[86] Two parallel HNLFs and a phase shifter were utilized to implement AO-NOT, XOR, and AND operations at 120 Gbps based on XPM effect as shown in Fig. 8. Here, the reconfigurability was achieved by slightly modifying the input signals and phase variation to obtain high quality output.[87] Ultrafast reconfigurable logic operations were numerically simulated based on a nonlinear metallodielectric grating with enhanced nonlinearity, high speed, and scalability in design with addition to compatibility with existing CMOS-based structures. Although the design provided sub-picosecond switching speeds with improved cascadability, the high switching power was still a limiting factor which required further improvement.[88] One of the earlier attempts involved an experimental demonstration of four different logic operations using an optical parametrical amplifier based on highly nonlinear dispersion shifted fibers working on FWM effect. AO-AND, NOT, XOR, and OR operations were achieved at 10 Gbps with possibility of operation up to 80 Gbps wherein reconfigurability was obtained by altering the input power, center frequencies, and/or polarization states on incoming signals.[89] By making use of the advantages of BPSK modulated signals such as nonlinearity tolerance and improved OSNR, photonic crystal MMI waveguides as shown in Fig. 9 attained AO-XOR, XNOR, OR, and NAND operations with high CR value. Different

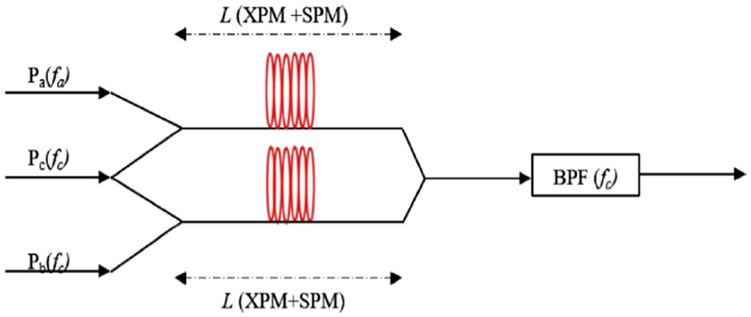

Fig. 8 Realization of reconfigurable AO-LGs using parallel HNLFs.[87]

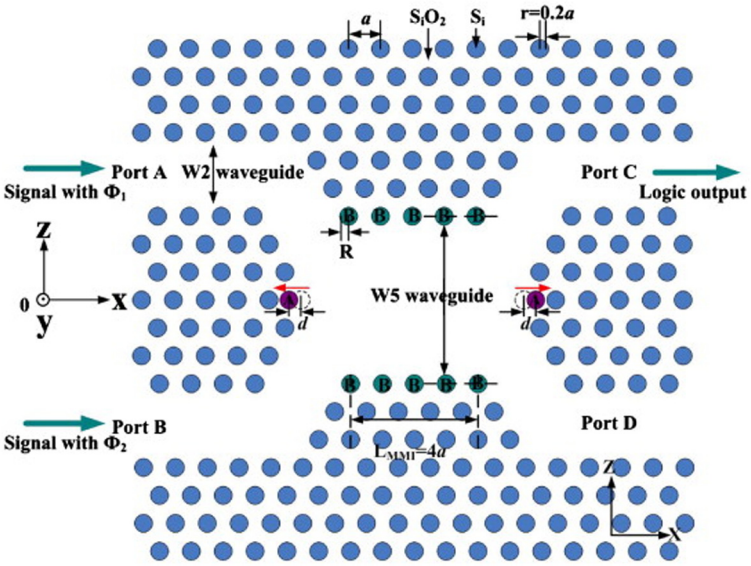

Fig. 9 Photonic crystal MMI-based structure for realizing attained AO-XOR, XNOR, OR, and NAND operations.[64]

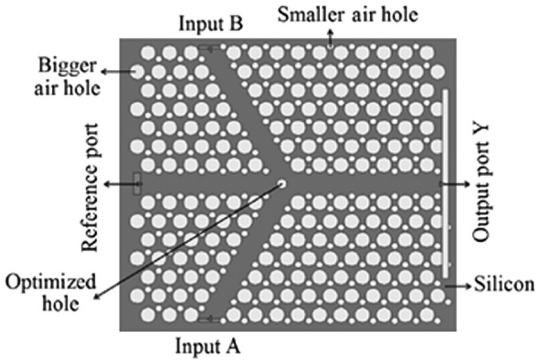

Fig. 10 Three-port honeycomb photonic crystal structure for reconfigurable AO-LG design.[90]

combinations of BPSK signals were used to realize the various logic operations without changing any structural parameters.[64] Reconfigurable and polarization independent AO-LGs were implemented on silicon on insulator photonic crystal structure with a complete bandgap in the 1550-nm optical window having a 2D honeycomb lattice structure as shown in Fig. 10. The reconfigurability was achieved by varying the phase angle of the reference signal within the three-port waveguide shaped structure.[90] An optical programmable Boolean logic unit has been designed using 2×2 polarization-independent optoelectronic cross bar switch. The above design is one of the first attempts at more complex reconfigurable structures capable of performing parallel switching operations with minimum data loss.[91] A summary of the design techniques for realizing reconfigurable AO-LGs is shown in Table 2.

Simultaneous AO-LGs achieve more than one logic operation within the same structure at the same time, i.e., when two or more logic functions are achieved simultaneously on different ports of a single device. The advantage of such gates compared with conventional ones is that they can achieve more than one logic function for the same set of input in the same device thereby saving space and lowering power requirements for an OIC. There have been designs for simultaneous AO-LG implementation in the recent times. AO-AND/OR operations were achieved simultaneously using incomplete coupling concept in nonlinear directional coupler with the aim of reducing power consumption and enabling cascaded operation.[92] A square lattice photonic crystal structure with two input and two output ports generated AO-OR and XOR output at each of the output ports at the same time. The proposed devices achieved control of light signals using

Table 2 Summary of reconfigurable AO-LGs.

Sl. no.	Logic function	Paper	Implementation	No. of reconfigurable logic functions achieved	Max CR (dB)	Max data rate	Footprint (μm^2)
1	AO-NOR, OR, AND	80	Experimental	3	—	100 Gbps	—
2	AO-AND, NOR, XOR, XNOR	81	Experimental	4	—	20 Gbps	—
3	AO-NOT, XOR	82	Simulation	2	43.4	3.15 Tbps	85.02
4	AO-XOR, OR	83	Simulation	2	—	—	150
5	6 basic LG functions + 19 advanced LG functions	84	Experimental + simulation	25	>6	10 Gbps	—
6	AO-AND, OR, XOR	85	Simulation	3	14	—	676
7	AO-AND, NOR, NOT, OR	86	Simulation	4	11.34	160 Gbps	—
8	AO-NOT, AND, XOR	87	Simulation	3	—	120 Gbps	—
9	AO-XOR, AND	88	Simulation	2	8	—	—
10	AO-XOR, OR, NOT, AND	89	Experimental	4	15.36	80 Gbps	—
11	AO-XOR, XNOR, NAND, OR	64	Simulation	4	28.6	—	46.23
12	AO-AND, OR, NOT, NAND, NOR, XNOR	90	Simulation	6	10	3.33 Tbps	—

line and point defects and operated with high data rate of 2.5 Tbps.[93] Another attempt to realize simultaneous AO-XOR/OR gates utilized a single quantum dot bimodal cavity working in the low-photon-number regime utilizing destructive interference effect.[94] Photonic crystal ring resonators utilizing the nonlinear Kerr effect was used to attain concurrent implementation of AO-XOR/AND gates at 746 Gbps with reduced power consumption at the telecommunication wavelength of 1550 nm.[95] The schematic for the same is shown in Fig. 11.

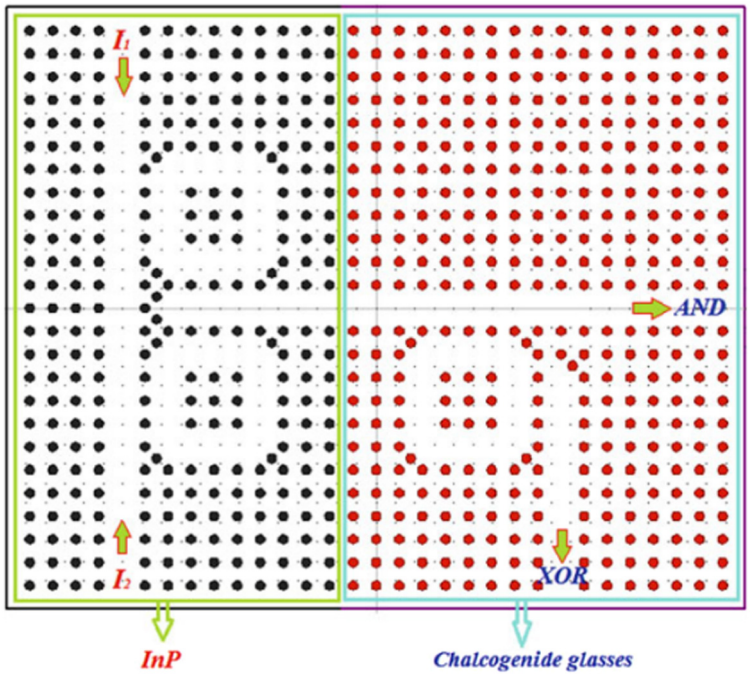

Fig. 11 Concurrent implementation of AO-XOR/AND using photonic crystal ring resonators.[94]

Table 3 Summary of simultaneous AO-LGs.

Sl. no.	Logic function	Paper	Implementation	No. of simultaneous logic functions achieved	Max CR (dB)	Max data rate	Footprint (μm^2)
1	AO-OR, AND	92	Simulation	2	—	500 Gbps	—
2	AO-XOR, OR	93	Simulation	2	6.76	2.5 Tbps	—
3	AO-OR, XOR	94	Simulation	2	—	—	—
4	AO-AND, XOR	95	Simulation	2	12.78	746 Gbps	320
5	AO-XOR, XNOR	96	Experimental	2	—	100 Mbps	—
6	AO-AND, OR	97	Simulation	2	17.95	6.76 Tbps	249.48
7	AO-XOR, NOR, OR, NAND	98	Experimental + simulation	4	10	10 Gbps	—
8	AO-XOR, XNOR	99	Simulation	2	—	—	1200
9	AO-XOR,AND	100	Simulation	2	14.13	—	—

Concurrent implementation of AO-XNOR/XOR was experimentally demonstrated at 100 Gbps using cascaded microring resonator-based electro-optic logic circuit using plasma dispersion effect. The proposed set up had limitations in improving the operating speed and lowering the dimensions which required further addressing.[96] Simultaneous AO-AND/OR logic function is attained with multiwavelength operation in the C band using a photonic crystal platform at ultrahigh bit rates.[97] An earlier attempt to achieve simultaneous implementation of AO-XOR, NOR, OR, and AND operations was experimentally demonstrated using two parallel SOA-MZI structures at 10 Gbps by suitable varying the gain and phase differences to attain maximum ER.[98] A nonlinear photonic crystal ring resonator-based structure was used to achieve simultaneous AO-XOR/XNOR operation at 1550 nm. However, the design possessed a higher footprint and longer response time, which required further improvement.[99] Simultaneous operation of AO-XOR and AND gates was achieved using one-dimensional periodic nonlinear material model with CR of 14.13 dB.[100] A 3×3 optical interconnecting switch based on QDSOA-MZI achieved three AO-logic operations simultaneously with high speed and CR of 8.20 dB.[101] Simultaneous AO-XOR/XNOR functions were realized using 2D MEMS-based diagonal switching with possible extension for higher bit operation.[102] A summary of the design techniques for realizing simultaneous AO-LGs is shown in Table 3.

4 Reversible AO-LGs

The literature considered so far involved only irreversible optical logic gates wherein the input bits are lost after generation of output bits. However, the conventional irreversible logic gates are not suitable for large-scale integrated circuits due to heat dissipation owing to bit loss at the output. Considering high-speed integrated circuits, a large amount of bit loss leads to a higher heat dissipation, which could lead to a serious issue. In such a scenario, the best option is to shift toward reversible logic gates. Reversible AO-LGs possess a direct mapping between input and output and there is no chance of bit loss, which lowers the heat dissipation in the circuit. The number of input ports and output ports remains the same leading to unique retrieval of input information from the output information. The use of reversible AO-LGs for the building optical processor leads to power efficient designs and improves the ability of data recovery. The main difference between reversible and irreversible logic gates is that reversible gates do not lose information, whereas irreversible gates tend to lose information after computation. Some of the widely used basic reversible gates in the electronic domain are Toffoli gate, Fredkin gate, and Feynman gate.

One of the initial attempts to demonstrate all-optical Fredkin gate utilized an SOA-based nonlinear loop mirror with a switching energy of 100 fJ.[103] Based on the nonlinear rotation of the state of polarization of probe beam and frequency conversion properties of nonlinear SOAs, frequency encoded AO-Fredkin and Toffoli gates were realized. The advantage of using frequency encoding to bring down the bit error problems along with high-bit-rate operation were achieved.[104] The attractive features of lithium niobate-based MZI structures, such as integration potential, thermal stability, compactness, low response time, and reconfigurability, were applied to realize AO-Fredkin and Feynman gates based on electro optic effect.[105] A different approach to design AO-Toffoli and Fredkin gates utilized the frequency conversion properties of SOA.[106] An attempt to construct a modified Fredkin gate using SOA-MZI structure with the ability to perform 15 Boolean logic functions was proposed. However, the proposed work was a preliminary model that needed further improvements to bring down the BER value and increase the speed of operation.[107] A plasmonics-based design approach was used to implement reversible NOT, swap, wire, and Feynman gates at 1550 nm. The above design used nanoring dielectric metal dielectric plasmonic waveguides based on interference effect.[108] AO-Fredkin gate was realized using photonic crystal based three types of nonlinear ring resonators with doped glass as nonlinear material.[109] AO-Feynman gate was theoretically analyzed and experimentally demonstrated using silicon microring resonators for 10 kbps.[110] A 16-wavelength hybrid AlGaInAs/InP microdisk laser array on silicon-on-insulator (SOI) was analyzed using FEM to improve the thermal characteristics for efficient operation.[111] A new design for reversible optical double Feynman gate using XPM in MZI was proposed for use in MZI-based quantum circuits.[112] An all-optical reversible programmable processor capable of performing 16 different operations was designed using liquid crystal-phase spatial light modulators, a polarization beam splitter, a half-wave plate, and plane mirrors.[113] SOA-assisted Sagnac interferometer-based design for the equalizer SWAP gate with improved performance in terms of reduced optical cost, low crosstalk, and high CR.[114] A simple design for all-optical Fredkin gate using mechanically controllable mirrors with feasibility for chip level implementation using MEMS was proposed.[115] All-optical Feynman, Toffoli, Peres, and Feynman double gates were realized using optically controlled bacteriorhodopsin protein-coated microresonators with low power consumption and high Q factor.[116]

The design of reversible AO-LGs is an upcoming area requiring wider research owing to its versatile areas of applications. It is the primary component required to design sequential and combination circuits for optical processors for applications, such as optical computing, optical signal processing, multivalues logic operations, and so on. The key advantages of such gates are low power consumption, high data recovery capabilities, least power dissipation, less hardware complexity, and high speed of operation. Hence, there is a growing need to design highly compact, flexible, and robust structures with high CR and low response times to achieve reversible logic operations. A summary of the design techniques for realizing all-optical reversible logic gates is shown in Fig. 12 and the details are tabulated in Table 4.

5 AO-LGs Based on Modulation Format and Data Rate

Another classification of AO-LGs is based on the modulation format of the input signals. A majority of the implementations makes use of on-off keying (OOK), as it can be directly

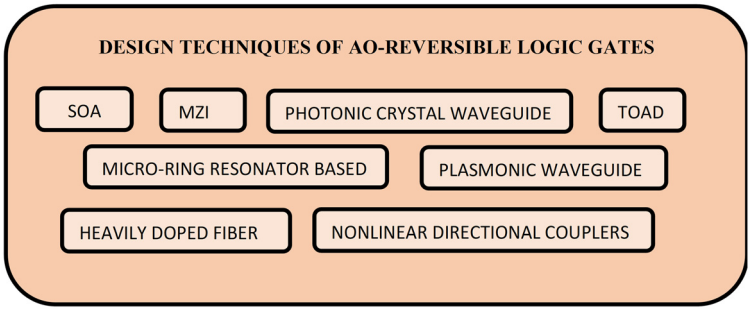

Fig. 12 Design techniques of AO-reversible LGs.

Table 4 Summary of reversible AO-LGs.

Sl. no.	Reversible AO-LG	Technique	Paper	Implementation
1	AO-Fredkin gate	SOA-based nonlinear loop mirror	103	Experimental
2	AO-Fredkin, Toffoli gate	SOA-based ADM	104	Numerical analysis
3	AO-Feynman, Fredkin gate	Lithium niobate-based MZI	105	Simulation
4	AO-Fredkin, Toffoli gate	SOA as PSW	106	Simulation
5	AO-modified Fredkin gate	SOA-MZI switch	107	Simulation
6	AO-Feynman gate	Plasmonic waveguides	108	Simulation
7	AO-Fredkin gate	Photonic crystal nonlinear cavities	109	Simulation
8	AO-Feynman gate	Silicon microring resonators	110	Experimental

interfaced with electrical logic without any encoding or decoding by merely switching the optical signal on and off. An investigation on AO-XOR operation between OOK and BPSK modulated signals was performed based on nonlinear effect in HNLF. The attempt was aimed to perform XOR operation on signals having different modulation formats without unnecessary conversion of signals to the same modulation format.[117] An experimental demonstration of dual channel AO-AND operation for OOK signals was achieved based on FWM using a fabricated multimode silicon waveguide.[118] FWM in a single SOA was utilized to obtain simultaneous implementation of AO-AND and OR operations for three different modulation formats at 40 Gbps.

A numerical analysis and experimental demonstration were performed for the typical NRZ-OOK format along with RZ-OOK (RZ) and CSRZ-OOK (carrier suppresses return to zero) formats with high ER values.[119] Another experimental demonstration for XOR operation was achieved using FWM effect in silicon nanowire for QPSK modulated signals with the capability of high-speed operation limited by the carrier recovery time.[120] A similar attempt using degenerate FWM in HNLF was utilized to obtain XOR operation for NRZ-DPSK signals at 40 Gbps with multicasting capability.[121] One of the earlier attempts to achieve AO-AND/OR operations for pulse position modulation (PPM) soliton pulses used a symmetric NLDC for TDM systems.[122] Another such design utilized integrated SOA-MZI to demonstrate AO-NAND operation at 10 Gbps which showed potential for further improved by utilizing differential scheme.[123] A summary of modulation format-based AO-LGs is tabulated in Table 5.

High data rate is one of the significant advantages offered by AO-LGs. An AO-AND gate operating at 10 Gbps was implemented and experimentally demonstrated using cascaded SOAs

Table 5 Summary of modulation format based AO-LGs.

Sl. no.	Logic function	Technique	Paper	Implementation	Modulation format used
1	AO-XOR	XPM in HNLF	117	Numerical analysis	OOK, BPSK
2	AO-AND	FWM in multimode silicon waveguide	118	Experimental	OOK
3	AO-OR, AND	FWM in SOA	119	Experimental	NRZ/RZ/CSRZ-OOK
4	AO-XOR	FWM in silicon nanowire	120	Experimental	QPSK
5	AO-XOR	FWM in HNLF	121	Experimental	NRZ-DPSK
6	AO-AND, OR	SPM in symmetric NLDC	122	Numerical analysis	PPM

based on XGM effect.[124] One of the first realizations of AO-XOR gate using NOLMs attained up to 10 Gbps speed.[125] Further experimental attempts based on UNI-[6] and SOA-based MZI configurations[126] achieved up to 20-Gbps data rate. To improve the data rate of AO-LGs based on SOA-MZI due to limitations imposed by carrier life time, a differential scheme was explored with potential capability of >100 Gbps operation.[127] A TOAD-based demultiplexer achieved 50 Gbps switching by exploiting the nonlinear effects in semiconductors with less than 1 pJ of energy as compared to earlier designs of AO-LGs.[128] A theoretical approach to accelerate the recovery time in SOA to achieve high data rates up to 2.5 Tbps with Q factor of 4.9 was utilized to design QD-SOA-based XOR gates.[129] An experimental demonstration of AO-AND gate using silicon microring resonator was performed at 10 Gbps attaining clear eye diagrams and low bit error rates.[130] A reconfigurable logic gate based on XPM in an HNLF was realized at 160 Gbps.[131] The major cause of low bit rate in XGM-based designs is the high chirping and lower ER values. These were overcome using high power pump signal with low power probe signal to realize various logic operations using XGM in SOA at a high bit rate of 340 Gbps.[132] A new scheme to realize AO-AND gate at 640 Gbps using a bulk SOA with turbo switch to boost the data rate using an improved version of differential scheme was numerically analyzed.[133] By utilizing the merits of both quantum dots and TPA effects, a shorter carrier recovery time and higher bit rates of 2 Tbps were attained for realizing AO-NOR and XNOR functions in QDSOAs.[134] A PCF-based NOLM was utilized to achieve AO-XNOR, XOR operations at 1 Tbps with lower dimensions and high ER values.[135] Another attempt at improving the data rate of QD-SOA-based AO-XOR gate without using MZI structure achieved 2 Tbps speed. The above work utilized nonMZI layout without any filter thereby lowering complexity and precise phase matching and tuning of filter.[136] A method to increase the data rate of a photonic crystal-based AND gate by changing diameter of hole increased the bit rate from 0.976 to 1.52 Tbit/s.[137] A summary of data rate-based AO-LGs is tabulated in Table 6.

Table 6 Summary of data rate-based AO-LGs.

Sl. no.	Logic function	Technique	Paper	Implementation	Data rate achieved
1	AO-AND	XGM in SOA	124	Experimental	10 Gbps
2	AO-XOR	Nonlinear effect in nonlinear loop mirror	125	Experimental	10 Gbps
3	AO-XOR	SOA-based UNI switch	6	Experimental	20 Gbps
4	AO-XOR	XGM in SOA-MZI	126	Experimental	20 Gbps
5	AO-XOR	XGM in QDSOA	129	Simulation	2.5 Tbps
6	AO-AND	Silicon microring resonator nonlinear effect	130	Experimental	10 Gbps
7	AO-XOR, OR, NAND, NOR, NOT	XPM in HNLF	131	Numerical analysis	160 Gbps
8	AO-NOT, XOR, XNOR, NOR	XGM in SOA	132	Simulation	340 Gbps
9	AO-AND	XGM in SOA-MZI	133	Numerical analysis	640 Gbps
10	AO-NOR, XNOR	Two photon absorption in QDSOA	134	Numerical analysis	2 Tbps
11	AO-XOR, XNOR	Photonic crystal fiber NOLM	135	Numerical analysis	1 Tbps
12	AO-XOR	XGM in QDSOA without filter	136	Numerical analysis	2 Tbps
13	AO-AND	Linear effect in photonic crystal waveguides	137	Simulation	1.52 Tbps

6 AO-Combinational and Sequential Logic Circuits

AO-LGs form the building blocks for the construction of various AO-combinational and sequential logic circuits for a wide variety of applications. Several AO-circuits such as code converters, parity checker and generator circuits, half adder, full adder, flip-flops (FFs), and so on are derived from basic AO-LGs as shown in Fig. 13. A brief review of such circuits and their methods of implementation is presented below.

6.1 *AO-Combinational Circuits*

A design of AO-Galois field adder based on a photonic crystal-based AO-XOR gate working on interference effect was proposed. The 4-bit adder was realized using 4 AO-XOR gates.[138] A design for 8 to 3 binary optical encoder utilized 4 AO-OR gates and a buffer gate to achieve efficient operation based on linear effects.[139] A structure for 4-to-2 AO-encoder based on a buffer and AO-OR gate utilized linear interference effect in 2D photonic crystals and achieved low response time.[140] Another such attempt was based on nonlinear effect in photonic crystal ring resonators and utilized AO-NOR gate.[141] An experimental demonstration of an AO-divider circuit based on AO-XOR gate for forward error detection was realized using SOA-MZI structures.[142] AO-half adder circuit based on AO-XOR/AND gates was proposed based on PhCRR with high CR and low footprint with operating wavelength of 1530 nm.[143] A similar attempt at realizing AO-half adder utilized AlGaAs is used as a nonlinear material and achieved maximum CR of 12.9 dB at 0.322 Tbps.[144] A photonic crystal semiconductor optical amplifier-Mach–Zehnder interferometer-based design of AO-half adder achieved high CR and data rate up to 500 Gbps.[145] AO-half adder and full adder circuits were realized using SOA-MZI utilizing nonlinear effects feasible for operation up to 60 Gbps.[146] A single SOA-based structure was used to

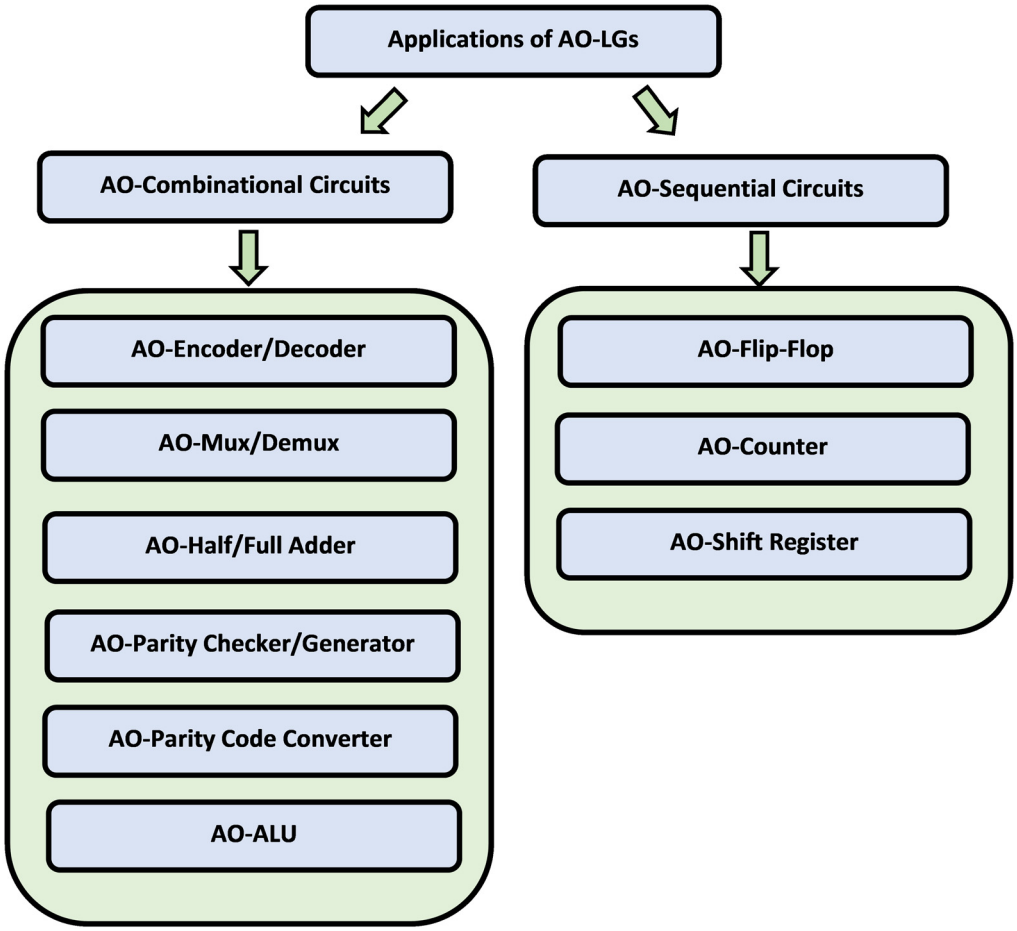

Fig. 13 Applications of AO-LGs.

realize half-subtracter, half-adder, comparator, and decoder with 10 Gbps operation based on FWM and XPM effects.[147] Frequency-encoded AO-XOR gate along with half adder and full adder circuits were implemented using a TOAD-based switch with acceptable CR value.[148] An AO-multifunctional logic circuit based on SOA-based polarization rotation switches enabled half adder, half subtractor, and comparator operations with high Q factor and 100 Gbps operating speed.[149] A plasmonic-based design approach of AO-half adder used SPP logic gates based on interference phenomena achieved small footprint and high CR.[150] Another plasmonic approach for realizing AO-full adder used MIM waveguides at 1550 nm with reduced losses and a transmission coefficient of 0.62.[151] A design of AO-comparator was proposed based on QD-SOA-based AO-AND, NO, XOR gates and achieved ER $>$ 10 dB and Q factor of 9 with high speed operation.[152] A structure for two's complement generator based on XOR gates was implemented based on RSOA with high Q factor and CR.[153]

A further step toward the use of the above circuits is constructing an AO-arithmetic and logic unit (ALU). One approach utilized seven MRR structures and beam splitter to achieve efficient operation without any optical crossings in the design shown in Fig. 14.[154] There have been several attempts utilizing to realize AO-ALU using SOA[155] and TOAD;[156] however, they possessed disadvantages such bulky dimensions and lack of integration capability for photonic integrated circuits (PICs).

Another application of AO-LGs is in the design of AO-code converters. Many types of binary codes, such as binary-coded decimal (BCD) codes, gray codes, and American Standard Code for Information Interchange, are used in digital systems. A code converter improves the efficiency of the overall signal-processing unit. A method to implement all-optical frequency-encoded gray code conversions using SOA-based polarization switches was proposed with operating speed up to 600 Gbps.[157] A 4-bit high-speed code converter utilizing two-photon absorption effect within microring resonators was designed at 1551 nm.[158] XGM in RSOA was used to realize an optical gray code converter with high Q factor at 1555 nm.[159] AO-binary-to-gray and gray-to-binary code converters were realized using linear interference effect in 2D photonic crystals to achieve good CR and low response time at 1550 nm.[160] AO-code converter based on SOA-MZI was used to perform binary-to-gray, BCD-to-gray, and octal-to-binary conversions at 500 Gbps.[161]

AO-parity checker and generator circuits are realized using AO-XOR/NOT gates for error correction and detection applications in computing and communication systems. A 3-bit AO-parity checker and generator was implemented using 4 MRRs to achieve a high CR of 15.56 dB.[162] Another attempt used AO-XOR gates based on linear interference of surface plasmon polaritons

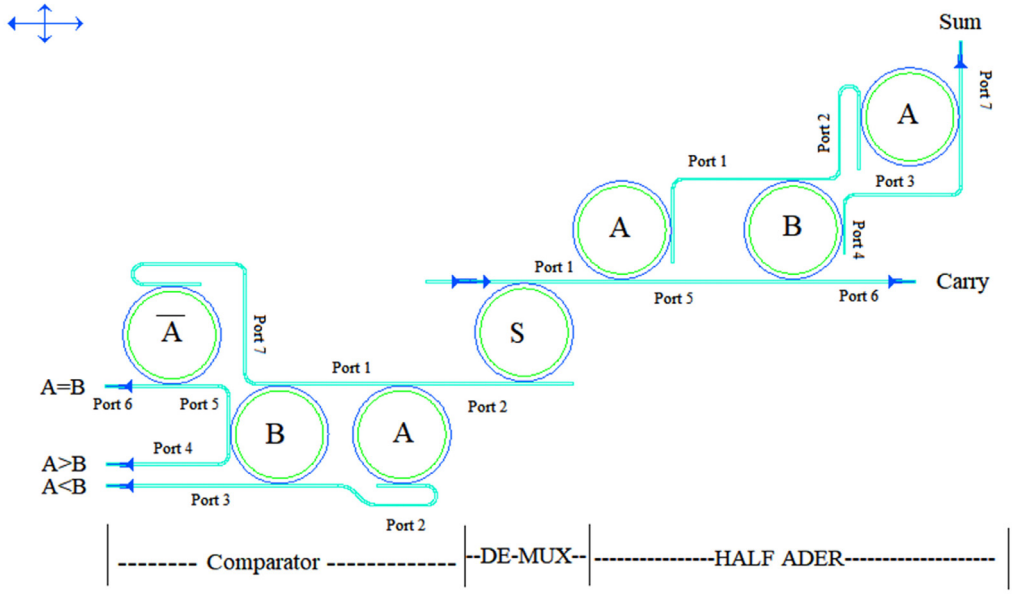

Fig. 14 Design of AO-ALU using MRRs.[154]

propagating in the plasmonic waveguides.[163] A 3-bit integrated AO-parity generator and checker circuit were realized using SOA-MZI-based optical tree architecture at 10 Gbps.[164]

6.2 *AO-Sequential Circuits*

AO-sequential circuits such as FFs, shift registers, and counters are realized using AO-LGs utilizing different techniques as detailed below. An AO-D FF was realized using MRRs with fast response time and small footprint.[165] Polarization rotation-based MRRs were utilized to realize AO-D, T FFs with cascaded layout possible for further extension.[166] A clocked D FF based on single GaAs-AlGaAs MRR achieved CR value of 16.53 dB.[167] AO-SR FF was realized using nonlinear Kerr effect in photonic crystal cavities with a device size of 361 μm^2 and maximum response time of 3.1 ps.[168] Optical MRR-based switch was utilized to achieve easy and cascadable structures for AO-JK, SR, and T FFs.[169]

A design of AO-D FF and 2-bit down counter was proposed based on nonlinear effect in optical MRR to achieve satisfactory performance metrics.[170] An AO-counter based on RS FF and AND gate was presented using cascaded stages of SOA fiber laser utilizing FWM effect.[171] Two-photon absorption effect in silicon MRR was used to achieve the design of CMOS compatible AO-RS FF and 2-bit counter at 45 Gbps.[172] An attempt to realize AO-two bit asynchronous up counter was proposed based on 2D PCRR-based RS FFs.[173] A 4-bit AO-synchronous up counter was designed using electro-optic effect in lithium niobate-based MZI.[174] An attempt to realize AO-Johnson counter was proposed utilizing XGM in SOA-based D FFs.[175]

AO-shift register have wide applications in optical packet buffers, serial-to-parallel converters, and synchronizers for all optical signal processing. A possible integrable structure for AO-shift register was proposed utilizing fiber loop-based AO-AND gate and optical buffer with multi-Gbps operation.[176] Silicon MRRs were used to realize AO-universal shift register using two optical multiplexers and two optical D FFs.[177]

7 Techniques/Principles for the Design of AO-LGs

The different methods of realizing various classifications of AO-LGs and their applications are covered in Secs. 2–6. Here, a summary of the various working principles involved in these designs are presented briefly.

(a) XPM: It arises when two or more different optical signals travel through a nonlinear medium. Due to the dependence of the refractive index on the intensity of light, refractive index nonlinearity converts the optical intensity fluctuations in one particular wavelength signal to phase variations in the copropagating signal. The nonlinear refractive index changes experienced by an optical beam depend not only on the intensity of that beam but also on the intensity of other copropagating beams.

(b) Cross gain modulation: A gain saturation process takes place within the SOA when both a probe signal and strong pump signal are applied to the SOA due to the high pump signal power. The gain of the probe is also modulated when the pump signal power is modulated with data. Thus, the data get transferred from the pump to probe as the probe signal output power is modulated.

(c) FWM: It is an intermodulation phenomenon in nonlinear optics wherein two beams of light at different operating wavelengths produce two new wavelengths or three wavelengths produce one new wavelength. It is a phase-sensitive process and is widely used in wavelength converters.[178]

(d) Linear interference effect: It occurs when two beams undergo interference in a linear medium. Constructive interference occurs when two beams interfere by a phase difference of $2k\pi$ (i.e., $k = 0, 1, 2...$) and destructive interference arises when two light signals have a phase difference of $(2k + 1)\ \pi$ (i.e., $k = 0, 1, 2...$).[179]

(e) Nonlinear Kerr effect: It is a nonlinear optical phenomenon that arises when light propagates in crystals and glasses. It is the change in refractive index caused by electric fields, the change being proportional to the square of electric field.[180]

(f) Plasmonic effect: It is the interaction between free electrons in metal nanoparticles and incident polarized light. Since light couples with the electrons, polarized light can be used to control the distribution of the electrons and the confinement of light occurs in a small dimension between metal and dielectric interface.[181]

8 CAD Tools for Simulation of AO-LGs

Various CAD-based simulation tools are utilized to investigate the light propagation and analyze the various performance metrics of AO-LGs. For most of the design techniques, experimental analysis becomes too expensive or lacks feasibility due to complexity or nonavailability of equipment/materials. Based on existing works, the commonly utilized simulation platforms for the study of AO-LGs are described briefly.

The RSoft CAD environment enables the design of various passive and active optical components and circuits to study in detail its various material properties and analyze light propagation within them using various modules, such as BandSOLVE, FullWAVE, and BeamPROP. The BandSOLVE module performs band gap calculations for 1D, 2D, and 3D photonic crystal devices using the PWE method. FullWAVE module utilizes FDTD method to perform a detailed analysis of the light propagation within the variety of photonic devices using high speed simulations. The BeamPROP tool is based on BPM to simulate and analyze the behavior of complex and integrated waveguide devices for a variety of applications, such as sensing, WDM, etc.[182] Another widely used simulation platform by researchers and engineers is COMSOL Multiphysics software for the modeling and analysis of devices in all areas of engineering with accurate results. There are a number of add-on modules corresponding to different fields of engineering, such as electromagnetics, structural mechanics, heat transfer, chemical engineering, and so on. The wave optics module under the section of electromagnetics modules has been widely used for the design of various optical components, such as waveguide couplers, plasmonic devices, optical fibers, photonic crystals, and so on. Several designs of AO-LGs based on photonic crystals, nonlinear effects, and plasmonic effects have been simulated using the above software with detailed analysis and accurate results.[183]

Optiwave Systems Inc. provides several products for photonic component level as well as system level design, simulation, optimization, and analysis for several research applications. The Optiwave Opti-FDTD software works on FDTD method to simulate various optical phenomena such as reflection, scattering, diffraction, polarization, and nonlinear effects in passive and nonlinear fiber optic components. It supports the testing and study of various components for applications such as CMOS sensor design, plasmonic designs, nanoparticle simulation, all-optical devices such as logic gates, couplers using photonic crystals, plasmonic waveguides, and so on.[184] The Optiwave Optisystem software enables system level analysis for realizing various integrated optical circuits for applications such as optical networks (WDM, OTDM, SONET/SDH rings, OCDMA etc.), free space optics, all-optical signal processing, radio over fiber (RoF), and so on. It utilizes numerical analysis or semianalytical techniques for systems limited by intersymbol interference and noise. Most of the SOA-based design of AO-LGs utilizing nonlinear effects have utilized the above software for simulation and analyzed various performance metrics with a system-level perspective.[185] For the analysis is of more complex waveguide devices, the Optiwave OptiBPM software based on BPM has been utilized. It has been used for several applications such as design of nonsymmetrical waveguide structures, couplers, splitters, sensor structures, rib or ridge waveguide design, and so on. Several designs of AO-LGs based on MZI have combined MATLAB with OptiBPM software to study the wave propagation within such structures.[186]

Another widely used simulation software for FDTD simulations is MIT electromagnetic equation propagation (MEEP), which is an open-source software developed at the Massachusetts Institute of Technology (MIT). It has been utilized to design photonic crystal-based all-optical devices, such as multiplexers, logic gates, splitters, and so on. Another similar open-source software for computing photonic band structures or dispersion relations of periodic dielectric structures is the MIT photonic bands (MPB).[187] Another highly efficient simulation tool for 2D/3D Maxwell's solver is Lumerical FDTD for the analysis and design of nanophotonic devices. It enables accurate modeling of photonic components for a broad range of applications, such

Table 7 Summary of the various CAD tools for simulation of AO-LGs.

Simulation tool	Modeling technique/method	Paper
RSoft CAD FullWAVE	FDTD	1, 54, 57, 60, 64, 65
RSoft CAD BandSOLVE	PWE	1, 54, 57, 59, 60
RSoft CAD BeamPROP	BPM	44 to 46
COMSOL Multiphysics	Physics-based modeling, equation-based modeling	68, 71, 72
Optiwave Opti-FDTD	FDTD	83
Optiwave Optisystem	Numerical analysis or semianalytical techniques	4, 5, 13, 17
Optiwave Opti-BPM	BPM	31
MEEP	FDTD	56, 66
MPB	PWE	56
Lumerical FDTD	FDTD	69

as surface plasmonics, photonic crystals, solar cells, metamaterials, and so on. A summary of the various CAD tools used for the design of AO-LGs is shown in Table 7.

9 Toward Photonic Integrated Circuits

In the current scenario, the existing communication systems are still operating on digital electronics and hybrid optoelectronic systems. However, due to the electronic bottle neck problem caused by the O/E/O conversions, there is a lack of complete utilization of optical transmission capacity of optical fibers in the existing fiber optic communication systems. Majority of the existing devices still require some O/E/O conversion for their operation and hence most of them are electro-optic devices and cannot be called all-optical devices. The idea of all-optical signal processing system/device requires all the operations to be performed completely in the optical domain without any conversions into electrical signals.

A truly optical system will consist of PICs similar to electronic integrated circuits wherein a large number of optical devices are integrated on a single chip.[188] A lot of research is being done on PICs in recent years to realize all-optical systems/devices.[189] With the evolution of PIC technology, many platforms have been developed such as SOI, SiN, InP, silica, and so on for specific requirements. PICs have attracted other applications beyond telecom/datacom, such as biomedical, Lidars, sensing, quantum processing, Lidars, 5G backhaul, among others.[190,191] Recently, silicon photonic integrated circuits have emerged as highly suitable candidates for all-optical systems owing to their ease of fabrication, ability for high density integration, and compatibility with the existing CMOS-based systems.[192] The two main platforms based on silicon for PICs are thin and thick SOI.

The selection of a suitable platform for PICs that can be used universally without compatibility issues is one of the existing challenges in the design of all-optical systems. Another challenge is the enabling of efficient coupling of light signals from the optical fiber backbone to the PICs. To overcome this issue, highly efficient and compatible coupling structures with compact dimensions and cost-effective fabrication need to be developed.[193,194] The design automation challenges associated with the integrated photonics device design also need further development. Some of the challenges that need to be addressed when moving from electronics to photonic design include the curvilinear layout, since photonic structures require smooth curves and bends for routing light to enable confinement; photonic circuit analysis capable of understanding the unique characteristics of photonic components; and new process design kits (PDKs) with additional features along with improved verification methodologies and tools.[195] Hence, to meet the

unique challenges of PIC design, dedicated photonic simulation and layout capabilities are needed.

10 Conclusion

AO-LGs are the crucial elements that play a pivotal role in various applications, such as all-optical computing, telecommunication, optical signal processing, and so on. Hence, the various design aspects of AO-LGs such as principle of operation, multiwavelength operation, power consumption, and miniaturization are of utmost interest to researchers and scientists working in various domains. The demand for high speed and miniaturization requires a fully optical integrated network with all-optical components, such as logic gates, encoders, decoders, and so on. The current requirement calls for all optical logic gates with high CR, low response times, reduced power consumption, small footprint, reversible operation, and flexible, robust designs with compatibility with hybrid electro-optic as well as fully OICs. The various classes of AO-LGs available in the literature are carefully reviewed and the research gaps are identified and concluded. Photonics and plasmonics are the current technologies driving the design of all-optical logic devices. Several other upcoming technologies such as topological photonics and AI-based designs have provided improved performances; however, their computation times, complexity, and practical implementation aspects need further studies.

Acknowledgments

This research did not receive any specific grants from funding agencies in the public, commercial, or not-for-profit sectors. The authors declare that they have no conflict of interest.

References

1. A. Mohebzadeh-Bahabady and S. Olyaee, "Designing low power and high contrast ratio all-optical NOT logic gate for using in optical integrated circuits," *Opt. Quantum Electron.* **51**, 3 (2019).
2. T. Durhuus et al., "High speed alloptical gating using two-section semiconductor optical amplifier structure," in *Proc. CLEO'92*, Anaheim, California, pp. 552–554 (1992).
3. H. Soto et al., "All-optical AND gate implementation using cross-polarization modulation in a semiconductor optical amplifier," *IEEE Photonics Technol. Lett.* **14**(4), 498–500 (2002).
4. K. Komatsu, G. Hosoya, and H. Yashima, "All-optical logic NOR gate using a single quantum-dot SOA-assisted an optical filter," *Opt. Quantum Electron.* **50**, 131 (2018).
5. J. M. Oliveira et al., "A new system for all-optical AND logic gate on semiconductor optical amplifier based Michelson," in *3rd Int. Symp. Instrum. Syst. Circuits and Transducers (INSCIT)*, pp. 1–6 (2018).
6. C. Bintjas et al., "20 Gb/s all-optical XOR with UNI gate," *IEEE Photonics Technol. Lett.* **12**(7), 834–836 (2000).
7. P. Singh et al., "Designs of all-optical buffer and OR gate using SOA-MZI," *Opt. Quantum Electron.* **46**, 1435–1444 (2014).
8. H. Sun et al., "All-optical logic XOR gate at 80 Gb/s using SOA-MZI-DI," *IEEE J. Quantum Electron.* **42**(8), 747–751 (2006).
9. A. Alquliah et al., "All-optical AND, NOR, and XNOR logic gates using semiconductor optical amplifiers-based Mach-Zehnder interferometer followed by a delayed interferometer." *Optik* **225**, 165901 (2021).
10. Y. Wang et al., "An all optical XOR logic gate for NRZ based on TOAD," in *PIERS Proc.*, Beijing, pp. 1286–1290 (2009).
11. T. Houbavlis et al., "10 Gbit/s all-optical Boolean XOR with SOA fibre Sagnac gate," *Electron. Lett.* **35**(19), 1650–1652 (1999).

12. C. Feng et al., "Simple ultrafast all-optical AND logic gate," *Opt. Eng.* **46**(12), 125006 (2007).
13. S. Saxena, S. Saxena, and S. Z. Rizvi, "Realization of all-optical NOR gate based on four wave mixing, non-linear effect in SOA," *Int. J. Latest Trends Eng. Technol.* **5**(1), 138–144 (2015).
14. A. Kotb, K. E. Zoiros, and W. Li, "Execution of all-optical Boolean OR logic using carrier reservoir semiconductor optical amplifier-assisted delayed interferometer," *Opt. Laser Technol.* **142**, 107230 (2021).
15. A. Kotb, K. E. Zoiros, and W. Li, "Realization of ultrafast all-optical NAND and XNOR logic functions using carrier reservoir semiconductor optical amplifiers," *J. Supercomput.* **77**, 14617–14629 (2021).
16. A. Kotb and C. Guo, "Numerical modeling of photonic crystal semiconductor optical amplifiers-based 160 Gb/s all-optical NOR and XNOR logic gates," *Opt. Quantum Electron.* **52**, 89 (2020).
17. M. Margarat et al., "All-optical XOR gate based on RSOA at 300 Gbps," in *Int. Conf. Syst. Comput. Autom. and Networking (ICSCAN)*, p. 1–6 (2021).
18. S. Ma et al., "High speed all optical logic gates based on quantum dot semiconductor optical amplifiers," *Opt. Express* **18**, 6417–6422 (2010).
19. S.-C. Mi et al., "Research of all-optical NAND gates based on quantum dot semiconductor optical amplifiers cascaded connection XGM and XPM," *Optik* **202**, 163551 (2020).
20. A. Kotb and K. E. Zoiros, "1 Tb/s high quality factor NAND gate using quantum-dot semiconductor optical amplifiers in Mach–Zehnder interferometer," *J. Comput. Electron.* **13**, 555–561 (2014).
21. X. Zhang and N. K. Dutta, "Effects of two-photon absorption on all optical logic operation based on quantum-dot semiconductor optical amplifiers," *J. Mod. Opt.* **65**(2), 166–173 (2018).
22. H. Taleb and K. Abedi, "Design of a low-power all-optical NOR gate using photonic crystal quantum-dot semiconductor optical amplifiers," *Opt. Lett.* **39**, 6237–6240 (2014).
23. A. Kotb, K. E. Zoiros, and C. Guo, "Ultrafast performance of all-optical AND and OR logic operations at 160 Gb/s using photonic crystal semiconductor optical amplifier," *Opt. Laser Technol.* **119**, 105611 (2019).
24. L. Vasundhara and S. Singh, "Implementation of XOR gate using a nonlinear polarization rotation in highly nonlinear fiber," in *Optical and Wireless Technologies*, Lecture Notes in Electrical Engineering, M. Tiwari et al., Eds., Vol. 771, Springer, Singapore (2022).
25. W. Wang et al., "Experimental research on 10 Gb/s all-optical logic gates with return-to-zero data in high nonlinear fiber," *Proc. SPIE* **8308**, 830829 (2011).
26. C. Yu et al., "All-optical XOR gate using polarization rotation in single highly nonlinear fiber," *IEEE Photonics Technol. Lett.* **17**(6), 1232–1234 (2005).
27. J. W. M. Menezes et al., "Logic gates based in two- and three-modes nonlinear optical fiber couplers," *Opt. Quantum Electron.* **39**, 1191–1206 (2007).
28. W. B. Fraga et al., "All optical logic gates based on an asymmetric nonlinear directional coupler," *Opt. Commun.* **262**(1), 32–37 (2006).
29. N. Trivunac-Vukovic, "Realization of all-optical ultrafast logic gates using triple core asymmetric nonlinear directional coupler," *J. Opt. Commun.* **22**(2), 59–63 (2001).
30. T. J. Xia et al., "All-optical packet-drop demonstration using 100-Gb/s words by integrating fiber-based components," *IEEE Photonics Technol. Lett.* **10**(1), 153–155 (1998).
31. A. Kumar, S. Kumar, and S. K. Raghuwanshi, "Implementation of XOR/XNOR and AND logic gates by using Mach–Zehnder interferometers," *Optik* **125**(19), 5764–5767 (2014).
32. Y.-D. Wu, T.-T. Shih, and M.-H. Chen, "New all-optical logic gates based on the local nonlinear Mach–Zehnder interferometer," *Opt. Express* **16**, 248–257 (2008).
33. S. Kumar and M. Sen, "Integrable all-optical NOT gate using nonlinear photonic crystal MZI for photonic integrated circuit," *J. Opt. Soc. Am. B* **37**, 359–369 (2020).
34. A. Araújo et al., "Two all-optical logic gates in a single photonic interferometer," *Opt. Commun.* **355**, 485–491 (2015).
35. M. R. Uddin, J. S. Cho, and Y. H. Won, "All-optical multicasting NOT and NOR logic gates using gain modulation in an FP-LD," *IEICE Electron. Express* **6**(2), 104–110 (2009).

36. L. Y. Chan et al., "All-optical bit error monitoring system using cascaded inverted wavelength converter and optical NOR gate," *IEEE Photonics Technol. Lett.* **15**(4), 593–595 (2003).
37. B. Nakarmi, M. Rakib-Uddin, and Y. H. Won, "Realization of all-optical multi-logic functions and a digital adder with input beam power management for multi-input injection locking in a single-mode Fabry–Pérot laser diode," *Opt. Express* **19**, 14121–14129 (2011).
38. J.-C. Liu et al., "Numerical simulation of all-optical logic gates based on hybrid-cavity semiconductor lasers," *J. Opt. Soc. Am. A* **38**, 808–816 (2021).
39. J. Wang, J. Sun, and Q. Sun, "Proposal for all-optical switchable OR/XOR logic gates using sum-frequency generation," *IEEE Photonics Technol. Lett.* **19**, 541–543 (2007).
40. J. Wang et al., "PPLN-based flexible optical logic and gate," *IEEE Photonics Technol. Lett.* **20**(3), 211–213 (2008).
41. Y. Zhang, Y. Chen, and X. Chen, "Polarization-based all-optical logic controlled-NOT, XOR, and XNOR gates employing electro-optic effect in periodically poled lithium niobate," *Appl. Phys. Lett.* **99**, 161117 (2011).
42. T. Chattopadhyay and D. K. Gayen, "Optical XOR-XNOR logic circuits using mechanical movable mirrors," in *2021 Devices for Integr. Circuit (DevIC)*, pp. 65–70 (2021).
43. A. Piccardi et al., "Soliton gating and switching in liquid crystal light valve," *Appl. Phys. Lett.* **96**, 071104 (2010).
44. S. Mohammadnejad, Z. F. Chaykandi, and A. Bahrami, "MMI-based simultaneous all-optical XOR–NAND–OR and XNOR–NOT multilogic gate for phase-based signals," *IEEE J. Quantum Electron.* **50**(12), 1–5 (2014).
45. Z. Farrokhi Chaykandi, A. Bahrami, and S. Mohammadnejad, "MMI-based all-optical multi-input XOR and XNOR logic gates using nonlinear directional coupler," *Opt. Quantum Electron.* **47**, 3477–3489 (2015).
46. J.-M. Kim et al., "Proposal of all-optical logic gate based on MMI," *Proc. SPIE* **5279**, 497–500 (2004).
47. Y. Fu et al., "All-optical logic gates based on nanoscale plasmonic slot waveguides," *Nano Lett.* **12**(11), 5784–5790 (2012).
48. K. J. A. Ooi et al., "Electro-optical graphene plasmonic logic gates," *Opt. Lett.* **39**, 1629–1632 (2014).
49. P. Sharma and V. D. Kumar, "All optical logic gates using hybrid metal insulator metal plasmonic waveguide," *IEEE Photonics Technol. Lett.* **30**(10), 959–962 (2018).
50. A. Pal, M. Z. Ahmed, and S. Swarnakar, "An optimized design of all-optical XOR, OR, and NOT gates using plasmonic waveguide," *Opt. Quantum Electron.* **53**, 84 (2021).
51. S. P. K. Anguluri et al., "The design, analysis, and simulation of an optimized all-optical AND gate using a Y-shaped plasmonic waveguide for high-speed computing devices," *J. Comput. Electron.* **20**, 1892–1899 (2021).
52. Y. Ishizaka et al., "Design of ultra compact all-optical XOR and AND logic gates with low power consumption," *Opt. Commun.* **284**(14), 3528–3533 (2011).
53. H. Wang, X. Yu, and X. Rong, "All-optical AND, XOR, and NOT logic gates based on Y-branch photonic crystal waveguide," *Opt. Eng.* **54**(7), 077101 (2015).
54. M. V. Sonth et al., "Basic logic gates in two dimensional photonic crystals for all optical device design," *Int. J. Electron. Telecommun.* **67**(2), 247–261 (2021).
55. F. Parandin, "Realization of ultra-compact all-optical universal NOR gate on photonic crystal platform," *J. Electr. Comput. Eng. Innov.* **9**(2), 185–192 (2021).
56. C. Tang et al., "Design of all-optical logic gates avoiding external phase shifters in a two-dimensional photonic crystal based on multi-mode interference for BPSK signals," *Opt. Commun.* **316**, 49–55 (2014).
57. A. Pashamehr, M. Zavvari, and H. Alipour-Banaei, "All-optical AND/OR/NOT logic gates based on photonic crystal ring resonators," *Front. Optoelectron.* **9**, 578–584 (2016).
58. M. Danaie and H. Kaatuzian, "Design and simulation of an all-optical photonic crystal AND gate using nonlinear Kerr effect," *Opt. Quantum Electron.* **44**, 27–34 (2012).
59. A. Kumar and S. Medhekar, "All optical NOR and NAND gates using four circular cavities created in 2D nonlinear photonic crystal," *Opt. Laser Technol.* **123**, 105910 (2020).

60. E. Veisi, M. Seifouri, and S. Olyaee, "A novel design of all-optical high speed and ultra-compact photonic crystal AND logic gate based on the Kerr effect," *Appl. Phys. B* **127**, 70 (2021).
61. R. Fan et al., "2D photonic crystal logic gates based on selfcollimated effect," *J. Phys. D: Appl. Phys.* **49**, 325104 (2016).
62. Y. Zhang, Y. Zhang, and B. Li, "Optical switches and logic gates based on self-collimated beams in two-dimensional photonic crystals," *Opt. Express* **15**, 9287–9292 (2007).
63. S. C. Xavier and K. P. Arunachalam, "Compact design of all-optical logic gates based on self-collimation phenomenon in two-dimensional photonic crystal," *Opt. Eng.* **51**(4), 045201 (2012).
64. W. Liu et al., "Design of ultra compact all-optical XOR, XNOR, NAND and OR gates using photonic crystal multi-mode interference waveguides," *Opt. Laser Technol.* **50**, 55–64 (2013).
65. E. H. Shaik and N. Rangaswamy, "Multi-mode interference-based photonic crystal logic gates with simple structure and improved contrast ratio," *Photonic Network Commun.* **34**, 140–148 (2017).
66. Y. Liu et al., "All-optical logic gates based on two-dimensional low-refractive-index nonlinear photonic crystal slabs," *Opt. Express* **19**, 1945–1953 (2011).
67. R. Yuan, C. Wang, and Z. Li, "Design of on-chip optical logic gates in 2D silicon photonic crystal slab," *Opt. Rev.* **27**, 277–282 (2020).
68. L. He et al., "Topologically protected beam splitters and logic gates based on two-dimensional silicon photonic crystal slabs," *Opt. Express* **28**, 34015–34023 (2020).
69. I. S. Maksymov, "Optical switching and logic gates with hybrid plasmonic–photonic crystal nanobeam cavities," *Phys. Lett. A* **375**(5), 918–921 (2011).
70. I. S. Amiri et al., "Realisation of all photonic logic gates using plasmonic-based photonic structure through bandgap analysis," *Optik* **194**, 163123 (2019).
71. J. M. Merlo et al., "All-optical logic gates based on anomalous Floquet photonic topological insulator structures," *J. Opt.* **23**, 065001 (2021).
72. L. He, W. X. Zhang, and X. D. Zhang, "Topological all-optical logic gates based on two-dimensional photonic crystals," *Opt. Express* **27**, 25841–25859 (2019).
73. Y. Wang et al., "Coherent interactions in one-dimensional topological photonic systems and their applications in all-optical logic operation," *Nano Lett.* **20**(12), 8796–8802 (2020).
74. V. Dhasarathan et al., "Realization of all logic gates using metamaterials based three-dimensional photonics structures: a future application of 3D photonics to optical computing," *Optik* **202**, 163723 (2020).
75. M. Ortiz-Martinez et al., "Logic gates for terahertz frequencies fabricated by three-dimensional printing," *J. Opt. Soc. Am. B* **37**, 3660–3664 (2020).
76. C. Qian et al., "Performing optical logic operations by a diffractive neural network," *Light Sci. Appl.* **9**, 59 (2020).
77. S. Hamedi and H. D. Jahromi, "Performance analysis of all-optical logical gate using artificial neural network," *Expert Syst. Appl.* **178**, 115029 (2021).
78. C.-E. Lin et al., "All optical XOR logic gate formed by unsupervised optical neuron networks," *Neurocomputing* **460**, 205–210 (2021).
79. K. E. Stubkjaer, "Semiconductor optical amplifier-based all-optical gates for high-speed optical processing," *IEEE J. Sel. Top. Quantum Electron.* **6**(6), 1428–1435 (2000).
80. X. Chen et al., "Study on 100-Gb/s reconfigurable all-optical logic gates using a single semiconductor optical amplifier," *Opt. Express* **24**(26), 30245–30253 (2016).
81. J. Xu et al., "Reconfigurable all-optical logic gates for multi-input differential phase-shift keying signals: design and experiments," *J. Lightwave Technol.* **27**(23), 5268–5275 (2009).
82. S. Olyaee et al., "Realization of all-optical NOT and XOR logic gates based on interference effect with high contrast ratio and ultra-compacted size," *Opt. Quantum Electron.* **50**, 385 (2018).
83. K. E. Muthu et al., "Design and analysis of a reconfigurable XOR/OR logic gate using 2D photonic crystals with low latency," *Opt. Quantum Electron.* **52**, 433 (2020).
84. X. Tang et al., "A reconfigurable optical logic gate with up to 25 logic functions based on polarization modulation with direct detection," *IEEE Photonics J.* **9**(2), 1–11 (2017).

85. R. E. Meymand, A. Soleymani, and N. Granpayeh, "All-optical AND, OR, and XOR logic gates based on coherent perfect absorption in graphene-based metasurface at terahertz region," *Opt. Commun.* **458**, 124772 (2020).
86. D. E. Fouskidis, K. E. Zoiros, and A. Hatziefremidis, "Reconfigurable all-optical logic gates (AND, NOR, NOT, OR) with quantum-dot semiconductor optical amplifier and optical filter," *IEEE J. Sel. Top. Quantum Electron.* **27**(2), 1–15 (2021).
87. L. Lovkesh, V. Sharma, and S. Singh, "The design of a reconfigurable all-optical logic device based on cross-phase modulation in a highly nonlinear fiber," *J. Comput. Electron.* **20**, 397–408 (2021).
88. A. Corbin and J.-T. Shen, "Ultrafast reconfigurable optical logic gates using a nonlinear metallodielectric grating," *Opt. Lett.* **46**, 2782–2785 (2021).
89. D. M. F. Lai, C. H. Kwok, and K. K.-Y. Wong, "All-optical picoseconds logic gates based on a fiber optical parametric amplifier," *Opt. Express* **16**, 18362–18370 (2008).
90. P. Rani, Y. Kalra, and R. K. Sinha, "Design and analysis of polarization independent all-optical logic gates in silicon-on-insulator photonic crystal," *Opt. Commun.* **374**, 148–155 (2016).
91. T. Chattopadhyay, "Optical programmable Boolean logic unit," *Appl. Opt.* **50**, 6049–6056 (2011).
92. E. Yaghoubi et al., "All optical OR/AND/XOR gates based on nonlinear directional coupler," *J. Opt.* **43**, 146–153 (2014).
93. K. Goudarzi et al., "All-optical XOR and OR logic gates based on line and point defects in 2-D photonic crystal," *Opt. Laser Technol.* **78**(Part B), 139–142 (2016).
94. H. Ye et al., "Simultaneous all-optical or and XOR logic gates based on the bimodal photonic cavity containing a quantum dot," *IEEE Photonics J.* **8**(6), 1–10 (2016).
95. M. Ghadrdan and M. A. Mansouri-Birjandi, "Concurrent implementation of all-optical half-adder and AND & XOR logic gates based on nonlinear photonic crystal," *Opt. Quantum Electron.* **45**, 1027–1036 (2013).
96. L. Zhang et al., "Electro-optic directed logic circuit based on microring resonators for XOR/XNOR operations," *Opt. Express* **20**, 11605–11614 (2012).
97. T. S. Mostafa, N. A. Mohammed, and E.-S. M. El-Rabaie, "Ultra-high bit rate all-optical AND/OR logic gates based on photonic crystal with multi-wavelength simultaneous operation," *J. Mod. Opt.* **66**(9), 1005–1016 (2019).
98. J.-Y. Kim et al., "All-optical multiple logic gates with XOR, NOR, OR, and NAND functions using parallel SOA-MZI structures: theory and experiment," *J. Lightwave Technol.* **24**, 3392–3399 (2006).
99. M. Asghari et al., "A novel proposal for all-optical XOR/XNOR gate using a nonlinear photonic crystal based ring resonator," *Opt. Appl.* **49**(2), 283–291 (2019).
100. T. Chattopadhyay, "All-optical simultaneous XOR-AND operation using 1-D periodic nonlinear material," *J. Opt. Commun.* (2021).
101. T. Chattopadhyay and D. K. Gayen, "Simultaneous all-optical multi logic operation using 3×3 interconnecting switch," *Opt. Fiber Technol.* **51**, 41–47 (2019).
102. T. Chattopadhyay, "2D MEMS based diagonal switching design for simultaneous optical XOR/XNOR operation," *Opt. Commun.* **330**, 6–11 (2014).
103. A. J. Poustie and K. J. Blow, "Demonstration of an all-optical Fredkin gate," *Opt. Commun.* **174**(1–4), 317–320 (2000).
104. S. K. Garai, "Novel method of designing all optical frequency-encoded Fredkin and Toffoli logic gates using semiconductor optical amplifiers," *IET Electron.* **5**(6), 247–254 (2011).
105. S. Kumar, Chanderkanta, and S. K. Raghuwanshi, "Design of optical reversible logic gates using electro-optic effect of lithium niobate based Mach–Zehnder interferometers," *Appl. Opt.* **55**, 5693–5701 (2016).
106. D. Mandal, S. Mandal, and S. K. Garai, "Alternative approach of developing all-optical Fredkin and Toffoli gates," *Opt. Laser Technol.* **72**, 33–41 (2015).
107. T. Chattopadhyay, "All-optical modified Fredkin gate," *IEEE J. Sel. Top. Quantum Electron.* **18**(2), 585–592 (2012).
108. M. N. Abbas and S. H. Abdulnabi, "Plasmonic reversible logic gates," *J. Nanophotonics* **14**(1), 016003 (2020).

109. M. Hassangholizadeh-Kashtiban et al., "All-optical Fredkin gate using photonic-crystal-based nonlinear cavities," *Appl. Opt.* **59**, 635–641 (2020).
110. Y. Tian et al., "Experimental demonstration of an optical Feynman gate for reversible logic operation using silicon micro-ring resonators," *Nanophotonics* **7**(1), 333–337 (2018).
111. S. Sui et al., "Sixteen-wavelength hybrid AlGaInAs/Si microdisk laser array," *IEEE J. Quantum Electron.* **51**(4), 1–8 (2015).
112. K. Bordoloi, T. Theresal, and S. Prince, "Design of all optical reversible logic gates," in *Int. Conf. Commun. and Signal Process.*, pp. 1583–1588 (2014).
113. T. Chattopadhyay, "Optical reversible programmable Boolean logic unit," *Appl. Opt.* **51**, 5266–5271 (2012).
114. T. Chattopadhyay, "An all-optical equalizer SWAP gate (ESG)," *Semicond. Sci. Technol.* **36**, 085017 (2021).
115. T. Chattopadhyay, "Negative controlled Fredkin gate circuits with mirrors," *IET Quantum Commun.* **3**(1), 60–71 (2022).
116. S. Roy et al., "All-optical reversible logic gates with optically controlled bacteriorhodopsin protein-coated microresonators," *Adv. Opt. Technol.* **2012**, 727206 (2012).
117. E. S. Nazemosadata and P. P. Shum, "All-optical XOR logic gate operating on inputs with different modulation formats," *Optik* **123**(22), 2028–2030 (2012).
118. J. Wang et al., "Dual-channel AND logic gate based on four-wave mixing in a multimode silicon waveguide," *IEEE Photonics J.* **9**(4), 1–6 (2017).
119. B. Wu et al., "Simultaneous implementation of all-optical OR and AND logic gates for NRZ/RZ/CSRZ ON–OFF-keying signals," *Opt. Commun.* **283**(3), 349–354 (2010).
120. Z. Yin et al., "All-optical logic gate for XOR operation between 40-Gbaud QPSK tributaries in an ultra-short silicon nanowire," *IEEE Photonics J.* **6**(3), 1–7 (2014).
121. J. Wang et al., "Experimental demonstration on 40Gbit/s all-optical multicasting logic XOR gate for NRZ-DPSK signals using four-wave mixing in highly nonlinear fiber," *Opt. Commun.* **282**(13), 2615–2619 (2009).
122. C. S. Sobrinho et al., "Analysis of an optical logic gate using a symmetric coupler operating with pulse position modulation (PPM)," *Opt. Commun.* **281**(5), 1056–1064 (2008).
123. X. Ye, P. Ye, and M. Zhang, "All-optical NAND gate using integrated SOA-based Mach–Zehnder interferometer," *Opt. Fiber Technol.* **12**(4), 312–316 (2006).
124. X. Zhang et al., "All-optical AND gate at 10 Gbit/s based on cascaded single-port-coupled SOAs," *Opt. Express* **12**, 361–366 (2004).
125. K. L. Hall and K. A. Rauschenbach, "All-optical bit pattern generation and matching," *Electron. Lett.* **32**(13), 1214–1215 (1996).
126. T. Fjelde et al., "Demonstration of 20 Gbit/s all-optical logic XOR in integrated SOA-based interferometric wavelength converter," *Electron. Lett.* **36**, 1863–1864 (2000).
127. Q. Wang et al., "Study of all-optical XOR using Mach-Zehnder interferometer and differential scheme," *IEEE J. Quantum Electron.* **40**(6), 703–710 (2004).
128. J. P. Sokoloff et al., "A terahertz optical asymmetric demultiplexer (TOAD)," *IEEE Photonics Technol. Lett.* **5**(7), 787–790 (1993).
129. A. Rostami et al., "Tb/s optical logic gates based on quantum-dot semiconductor optical amplifiers," *IEEE J. Quantum Electron.* **46**(3), 354–360 (2010).
130. M. Xiong et al., "All-optical 10 Gb/s AND logic gate in a silicon microring resonator," *Opt. Express* **21**, 25772–25779 (2013).
131. A. Bogris, P. Velanas, and D. Syvridis, "Numerical investigation of a 160-Gb/s reconfigurable photonic logic gate based on cross-phase modulation in fibers," *IEEE Photonics Technol. Lett.* **19**(6), 402–404 (2007).
132. L. Lovkesh, V. Sharma, and S. Singh, "340 Gb/s all-optical NOT, XOR, XNOR, $A^{-}B$, AB^{-}, OR and NOR logic gates based on cross-gain modulation in semiconductor optical amplifiers," *Optik* **247**, 168016 (2021).
133. I. Rendón-Salgado, E. Ramírez-Cruz, and R. Gutiérrez-Castrejón, "640 Gb/s all-optical AND gate and wavelength converter using bulk SOA turbo–switched Mach–Zehnder interferometer with improved differential scheme," *Opt. Laser Technol.* **109**, 671–681 (2019).

134. A. Kotb and C. Guo, "All-optical NOR and XNOR logic gates at 2 Tb/s based on two-photon absorption in quantum-dot semiconductor optical amplifiers," *Opt. Quantum Electron.* **52**, 1–19 (2019).
135. S. Sharma and J. Kumar, "Numerical analysis of optical logic gate based on nonlinear optical loop mirror with a photonic crystal fiber," *J. Nonlinear Opt. Phys. Mater.* **24**(2), 1550019 (2015).
136. K. Mukherjee, "Non-MZI all-optical XOR gate using cross-gain modulation in quantum dot semiconductor optical amplifier at 2 Tb/s without filter," *J. Opt.* **50**, 535–541 (2021).
137. R. Dayhool and A. R. Maleki Javan, "New method to improve bit-rate of all-optical logic gate based on 2D photonic crystal," *Optik* **183**, 591–594 (2019).
138. A. Andalib, "A novel proposal for all-optical Galois field adder based on photonic crystals," *Photonics Network Commun.* **35**, 392–396 (2018).
139. S. Naghizade, S. Mohammadi, and H. Khoshsima, "Design and simulation of an all optical 8 to 3 binary encoder based on optimized photonic crystal OR gates," *J. Opt. Commun.* **42**(1), 31–41 (2021).
140. M. Soroosh, H. Alipour-Banaei, and F. Mehdizadeh, "A proposal for 4-to-2 optical encoder based on photonic crystals," *IET Optoelectron.* **11**(1), 29–35 (2017).
141. T. A. Moniem, "All-optical digital 4 × 2 encoder based on 2D photonic crystal ring resonators," *J. Mod. Opt.* **63**(8), 735–741 (2016).
142. Y. Aikawa, S. Shimizu, and H. Uenohara, "Demonstration of all-optical divider circuit using SOA-MZI-type XOR gate and feedback loop for forward error detection," *J. Lightwave Technol.* **29**, 2259–2266 (2011).
143. F. Parandin and M. Reza Malmir, "Reconfigurable all optical half adder and optical XOR and AND logic gates based on 2D photonic crystals," *Opt. Quantum Electron.* **52**, 56 (2020).
144. P. Sami, C. Shen, and M. H. Sani, "Ultra-fast all optical half-adder realized by combining AND/XOR logical gates using a nonlinear nanoring resonator," *Appl. Opt.* **59**, 6459–6465 (2020).
145. M. Margarat et al., "PCSOA-MZI based all-optical half adder," in *6th Int. Conf. Commun. Electron. Syst. (ICCES)*, pp. 222–228 (2021).
146. M. Ramachandran, S. Prince, and D. Verma, "Design and performance analysis of all-optical cascaded adder using SOA-based MZI," *J. Comput. Electron.* **17**, 845–856 (2018).
147. Y. Liu et al., "All-optical non-inverted half-subtracter, half-adder, comparator, and decoder simultaneously based on a single semiconductor optical amplifier," *Opt. Eng.* **60**(7), 076106 (2021).
148. K. Mukherjee et al., "TOAD-based frequency-encoded all optical XOR gate, half adder, and half subtractor," in *Emerging Trends in Terahertz Engineering and System Technologies*, A. Biswas et al., Eds., Springer, Singapore (2021).
149. A. Raja, K. Mukherjee, and J. N. Roy, "Design analysis and applications of all-optical multifunctional logic using a semiconductor optical amplifier-based polarization rotation switch," *J. Comput. Electron.* **20**, 387–396 (2021).
150. T. Birr et al., "Ultrafast surface plasmon-polariton logic gates and half-adder," *Opt. Express* **23**, 31755–31765 (2015).
151. M. Olyaee et al., "Propose, analysis and simulation of an all optical full adder based on plasmonic waves using metal-insulator-metal waveguide structure," *J. Optoelectron. Nanostruct.* **4**(3), 95–116 (2019).
152. K. Komatsu, G. Hosoya, and H. Yashima, "Ultrafast all-optical digital comparator using quantum-dot semiconductor optical amplifiers," *Opt. Quantum Electron.* **51**, 39 (2019).
153. K. Mukherjee, K. Maji, and A. Raja, "All optical four bit two's complement generator and single bit comparator using reflective semiconductor optical amplifier," *Int. J. Nano Biomater.* **9**(1-2), 64–79 (2020).
154. N. B. Jadhav et al., "Micro-ring resonator based all-optical arithmetic and logical unit," *Optik* **244** (2021).
155. S. K. Garai, "A novel all-optical frequency-encoded method to develop arithmetic and logic unit (ALU) using semiconductor optical amplifiers," *J. Lightwave Technol.* **29**, 3506–3514 (2011).

156. J. N. Roy and D. K. Gayen, "Integrated all-optical logic and arithmetic operations with the help of a TOAD-based interferometer device: alternative approach," *Appl. Opt.* **46**, 5304–5310 (2007).
157. S. K. Garai, "Method of all-optical frequency encoded decimal to binary and binary coded decimal, binary to gray, and gray to binary data conversion using semiconductor optical amplifiers," *Appl. Opt.* **50**(21), 3795–807 (2011).
158. G. K. Bharti and J. K. Rakshit, "Design and performance analysis of high speed optical binary code converter using micro-ring resonator," *Fiber Integr. Opt.* **37**(2), 103–121 (2018).
159. K. Mukherjee, K. Maji, and A. Raja, "All-optical Feynman gate using reflective semiconductor optical amplifiers and binary to gray code converter," *Adv. Appl. Math. Sci.* **19**(9), 919–929 (2019).
160. E. G. Anagha and R. K. Jeyachitra, "Investigations on all-optical binary to gray and gray to binary code converters using 2D photonic crystals," *IEEE J. Quantum Electron.* **57**(6), 1–10 (2021).
161. M. Michael, B. E. Caroline, and S. C. Xavier, "M-ary DPSK coded binary to gray, BCD to gray, and octal to binary all-optical code converters based on SOA-MZI configuration at 500 Gb/s," *Appl. Opt.* **59**, 8126–8135 (2020).
162. J. K. Rakshit, J. N. Roy, and T. Chattopadhyay, "Design of micro-ring resonator based all-optical parity generator and checker circuit," *Opt. Commun.* **303**, 30–37 (2013).
163. F. Wang et al., "Nanoscale on-chip all-optical logic parity checker in integrated plasmonic circuits in optical communication range," *Sci. Rep.* **6**, 24433 (2016).
164. N. Nair, S. Kaur, and R. Goyal, "All-optical integrated parity generator and checker using an SOA-based optical tree architecture," *Curr. Opt. Photonics* **2**, 400–406 (2018).
165. A. Kumar and S. K. Raghuwanshi, "Implementation of some high speed combinational and sequential logic gates using micro-ring resonator," *Optik* **127**(20), 8751–8759 (2016).
166. G. K. Bharti and R. K. Sonkar, "Design and performance analysis of all-optical D and T flip-flop in a polarization rotation based micro-ring resonator," *Opt. Quantum Electron.* **54**, 176 (2022).
167. J. K. Rakshit, J. N. Roy, and T. Chattopadhyay, "A theoretical study of all optical clocked D flip flop using single micro-ring resonator," *J. Comput. Electron.* **13**, 278–286 (2014).
168. S. S. Zamanian-Dehkordi, M. Soroosh, and G. Akbarizadeh, "An ultra-fast all-optical RS flip-flop based on nonlinear photonic crystal structures," *Opt. Rev.* **25**, 523–531 (2018).
169. G. K. Bharti and J. K. Rakshit, "Design of all-optical JK, SR and T flip-flops using micro-ring resonator-based optical switch," *Photonics Networks Commun.* **35**, 381–391 (2018).
170. N. Verma and D. Mishra, "New approach to design D-flip flop and two bit down counter using optical micro-ring resonator for high speed data processing," *SN Appl. Sci.* **2** 542 (2020).
171. J. Wang et al., "All-Optical counter based on optical flip-flop and optical AND gate," in *35th Eur. Conf. Opt. Commun.*, pp. 1–2 (2009).
172. P. Sethi and S. Roy, "Ultrafast all-optical flip-flop and binary counter using silicon micro-ring resonators," in *12th Int. Conf. Fiber Opt. and Photonics*, OSA Technical Digest, Optica Publishing Group (2014).
173. T. A. Moniem, "A two bit optical counter using integrated 2D square lattice photonic crystals," *Opt. Quantum Electron.* **48**, 424 (2016).
174. S. Kumar et al., "An optical synchronous up counter based on electro-optic effect of lithium niobate based Mach–Zehnder interferometers," *Opt. Quantum Electron.* **47**, 3613–3626 (2015).
175. S. Singh et al., "Photonic processing of all-optical Johnson counter using semiconductor optical amplifiers," *IET Optoelectron.* **11**, 8–14 (2017).
176. S. Kaur and R. S. Kaler, "All-optical circular shift register based on semiconductor optical amplifiers," *Opt. Quantum Electron.* **46**, 991–998 (2014).
177. J. K. Rakshit and J. N. Roy, "Design of all-optical universal shift register using nonlinear microring resonators," *J. Comput. Electron.* **15**, 1450–1461 (2016).
178. G. Keiser, *Optical Fiber Communications*, 4th ed., McGraw Hill, New York (2007).

179. A. Safinezhad et al., "High-performance and ultrafast configurable all-optical photonic crystal logic gates based on interference effects," *Opt. Quantum Electron.* **53**, 259 (2021).
180. M. Shirdel and M. A. Mansouri-Birjandi, "Photonic crystal all-optical switch based on a nonlinear cavity," *Optik* **127**(8), 3955–3958 (2016).
181. Z. Zalevsky and I. Abdulhalim, "*Chapter 6 – Plasmonics, Integrated Nanophotonic Devices*, 2nd ed., pp. 179–245, William Andrew Publishing (2014).
182. "RSoft photonic device tools," https://www.synopsys.com/photonic-solutions/rsoft-photonic-device-tools.html.
183. "COMSOL Multiphysics® Simulation software," https://www.comsol.com/comsol-multiphysics.
184. "OptiFDTD overview," https://optiwave.com/optifdtd-overview/
185. "OptiSystem overview," https://optiwave.com/optisystem-overview/
186. "OptiBPM overview," https://optiwave.com/optibpm-overview/
187. "MPB-MIT photonic bands," http://abinitio.mit.edu/wiki/index.php/MIT_Photonic_Bands
188. X. Ji et al., "Compact, spatial-mode-interaction-free, ultralow-loss, nonlinear photonic integrated circuits," *Commun. Phys.* **5**, 84 (2022).
189. C. Shang et al., "Perspectives on advances in quantum dot lasers and integration with Si photonic integrated circuits," *ACS Photonics* **8**(9), 2555–2566 (2021).
190. G. B. de Farias et al., "How to develop your product based on photonic integrated circuits technologies," in *SBFoton Int. Opt. and Photonics Conf. (SBFoton IOPC)*, pp. 1–3 (2021).
191. T. K. Paraïso et al., "A photonic integrated quantum secure communication system," *Nat. Photonics* **15**, 850–856 (2021).
192. X. Shen et al., "Silicon photonic integrated circuits and its application in data center," *Proc. SPIE* **11763**, 1176380 (2021).
193. W. S. Zaoui et al., "Bridging the gap between optical fibers and silicon photonic integrated circuits," *Opt. Express* **22**, 1277–1286 (2014).
194. X. Mu et al., "Edge couplers in silicon photonic integrated circuits: a review," *Appl. Sci.* **10**(4), 1538 (2020).
195. J. Pond, G. S. C. Lamant, and R. Goldman, "Chapter 5 – Software tools for integrated photonics," in *Optical Fiber Telecommunications VII*, A. E. Willner, Ed., pp. 195–231, Academic Press (2020).

Erandathara Gokulan Anagha received her master's of engineering degree in communication systems from Vellore Institute of Technology, Vellore, Tamil Nadu, India, in 2018. She is currently working toward her PhD at the Department of Electronics and Communication Engineering, National Institute of Technology, Tiruchirappalli, India. Her research interests include all-optical devices, photonics, and optical communication.

Ramasamy Kandasamy Jeyachitra received her master's of engineering degree in microwaves and optical engineering from Alagappa Chettiar College of Engineering and Technology, Karaikudi, Tamil Nadu, India, and her PhD in information and communication engineering from Anna University, Chennai. In 2007, she joined the National Institute of Technology (NIT), Trichy, India, where she is now an associate professor in the Department of Electronics and Communication Engineering. She has several years of research experience in the areas of advanced communication systems. Her research interests include information and communication systems, microwave/millimeter-wave photonics, optical wireless communication, RoF, optical communication, artificial intelligence in optical communication, optical logic gates, and PCFs. She is a life member of the Institution of Engineers (IE), Indian Institution of Electronics and Telecommunication Engineers (IETE), and Indian Society for Technical Education (ISTE). She has reviewed books and acted as a reviewer for several refereed international journals, such as *IEEE MTT*, *IEEE Access*, *IEEE Communication Letters*, and *Springer Telecommunications*. She also serves on the technical program committee for IEEE international conferences.